Anti-CSC effect of NADPH oxidase inhibitors

SADIA MONZUR

Student ID: 7501102

Doctoral degree Project

Interdisciplinary science and Engineering in Health system, Okayama University

Spring term 2022

Supervisor: Professor Masaharu Seno

Popular Scientific summary

Cancer stem cells (CSCs) are the leading players of all neoplastic systems, which are characterized by their self-renewal capacity, pluripotency, metastasis, heterogeneity, multidrug resistance, and low proliferation rate. These characteristic features have been designated as the sole causes of cancer relapse. With the experimental validation of CSCs, the understanding of cancer has changed significantly over the last two decades. CSC characteristic features like cellular hierarchy, the role of CSCs in the tumor niche, regulation of the biological activity, abnormal metabolism, immune interactions, and drug resistance. Understanding the key features of CSCs is essential to paint a clearer picture of carcinogenesis progression, which can help us formulate strategies to eradicate this subpopulation. Reactive oxygen species have been implicated in the etiology of many human diseases, including cancer. Their function in developing and maintaining cancer stem cells is not well understood yet. But considering their role in cancer recurrence and chemo- and radio-resistance, this seems to be one of the most critical research areas in current oxidative medicine.

Nicotinamide adenine dinucleotide phosphate (NADPH Oxidase) is a superfamily of enzymes consisting of 5 members NOX1, NOX2, NOX3 NOX4, NOX5, DUOX1, and DUOX2. They have been known to be critical producers of ROS. Out of the seven members of the NOX family, NOX1, NOX2, NOX3, and NOX5 are transmembrane proteins that function to transport electrons across biological membranes to reduce oxygen superoxide. At the same time, NOX4, DUOX1, and DUOX2 are hydrogen peroxide (H_2O_2) producers. Cellular reactive oxygen species (ROS) such as hydrogen

peroxide (H2O2) and superoxide anion (O_2 •−) are generally produced in response to cytokine or growth factor stimuli or as a by-product of mitochondrial oxidative phosphorylation. These ROS molecules play the role of secondary messengers involved in regulating cell differentiation, growth, migration, and host defense. However, these enzymes can also be mediators of oxidative stress, apoptosis, migration hypertension, fibrosis. Cellular proliferation and angiogenesis. I hypothesized in this study that complete or partial blockage of NOX activity would affect the mitochondrial respiration of CSCs resulting in significant energy depletion showcasing anti-CSC effects. In this dissertation, I evaluated the small molecule NOX inhibitors NOX inhibitors Apocynin, Diphenyleneiodonium chloride (DPI), GLX7013144, GLX7012166, and VAS2870 to target metabolic pathways in CSCs. Of the drug mentioned above, only Diphenyleneiodonium chloride showed an anti-CSC effect on the cancer stem cells derived from miPS cells designated as miPS-Huh7cmP cells on MTT assay. Even though DPI has long been evaluated as an anti-cancer drug inhibiting NADPH oxidase, the IC 50 in several cancer cell lines was reported to be 10 μM, which is too high for efficacy. This study employed miPS-Huh7cmP cells, which we previously established as a cancer stem cell (CSC) model. We found the cells from a primary culture of a tumor developed in a nude mouse when miPSCs treated with the conditioned medium of human hepatocarcinoma cell line Huh7 cells were transplanted. I re-evaluated the efficacy of DPI using this CSC model because CSCs are currently one of the main foci of therapeutic strategies to treat cancer but are generally considered resistant to chemotherapy. As a result, the conventional assay for the cell growth inhibition by DPI

accounted for an IC50 at 712 nM that was not enough to define the effectiveness as an anti-CSC drug. Simultaneously, the wound healing assay revealed an IC50 of approximately 500 nM. Comparatively, the IC50 values shown on sphere formation, colony formation, and tube formation assays were 5.5, 12 and 8.7 nM, respectively. However, these inhibitory effects were not observed by VAS2780, also a reputed NADPH oxidase inhibitor. It is noteworthy that these three assays evaluate the characteristics of CSCs designed in the 3D culture. Since the anti-CSC effect of DPI has successfully demonstrated on the liver CSC model, I developed the glioblastoma stem cell model using miPSCs to assess the efficacy of DPI on other CSC models. miPS cells were treated with the conditioned medium of human glioblastoma cell lines A172, GI1, and U251MG cells. Out of the 3 types of condition media, those from A172 and U251MG cells effectively prepared the cells with characteristics of CSCs. Considering that the markers of neuro-phenotype are positive on the obtained cells, the establishment of glioblastoma stem cells could be retained shortly.

Table of contents

Chapter One: General Introduction

Abstract

Cancer stem cells (CSCs) are the leading players of all neoplastic systems, characterized by their self-renewal capacity, pluripotency, metastasis, heterogeneity, multidrug resistance, and low proliferation rate. These characteristic features have been designated as the sole causes of cancer relapse. With the experimental validation of CSCs, the understanding of cancer has been changed significantly over the last two decades. In this paper, we briefly review the literature emphasizing six essential points that will allow us to understand the CSCs in a nutshell. These include CSC's characteristic features like cellular hierarchy, the role of CSCs in the tumor niche, regulation of the biological activity, abnormal metabolism, immune interactions, and drug resistance. Describing the critical features of CSCs will allow us to paint a somewhat more precise picture of carcinogenesis progression, which can help us formulate strategies to eradicate this subpopulation. Thus, providing a solution to the problem of drug resistance and metastasis of cancer in the future.

Keywords

Cancer stem cells, CSC cellular hierarchy, CSC tumor niche, CSC metabolism, CSC immune escape, CSC drug resistance

Introduction

Cancer is the uncontrolled growth of abnormal cells in the human body. This unchecked growth happens when the body's normal control mechanism stops working. Cancer can involve any body tissue and have many different forms in each body area. In the 21st century, cancer is the world's second leading cause of death. The IARC Global Cancer Observatory reported in 2018 that the global tumor burden had been estimated to rise to 18.1 million, and the Abdullah death toll due to cancer is 9.6 million. Due to the high rate of population growth, aging, and distribution of risk factors associated with socioeconomic development, it is estimated that there will be 29 million new cases of cancer by 2030[1, 2]. Although millions have been invested in this field both by government and private authorities, still to this day, approaches to treat cancer patients give the outcome of 1- or 5-year relative survival rate, depending on the metrics that are relevant at a particular point in follow-up time after diagnosis[3]. Tumors are composed of different types of cancer cells that contribute to tumor heterogeneity. CSCs play a significant role in cancer initiation and progression between these populations of cells. This CSCs were first recognized in leukemia using the experimental xenotransplantation procedure[4]. CSCs have now been identified in many other malignancies from this early discovery. CSCs (CSCs) exist within the tumor niche, varying in frequencies which range around 0.02% to 25% depending on the type of the tumor, where higher CSC proportions are found in undifferentiated tumors [5, 6, 7.] Usually, upper CSC rates are found in leukemias and lymphomas, while lower rates are normally found in solid tumors. CSCs hold potential for long-term self-renewal and differentiation, making CSCs unique compared to other neoplastic cells [8]. The CSC term

was first coined in 1959 to explain cancer relapse by Makino[9, 10]. Various studies reported that the heterogeneous tumor could be achieved by xenografting a small number of cells into immune-deficient mice. However, efforts to characterize these cells began only in the early 1990s [11, 12, 13]. In 1994, Dick was the first who demonstrated the strength of these CSCs in Acute Myeloid Leukemia (AML) by pointing out that CD34+ and CD38- cells comprised 1% of the tumor mass. As low as only 5000 cells from this subpopulation were able to form tumors in mice, these are the leading players of all neoplastic systems and are the sole reason for cancer relapse[14, 15, 16]. Following this report, these tumor-initiating, drug-resistant, and stemness-activated cells have been identified in different types of cancers like ovarian cancer[17] breast[18], colon[19], pancreatic[20], liver, stomach cancers[21], glioblastoma[22], melanoma[23] and other types of cancer. Metastasis potential is of the characteristic features of the CSCs, and this process is also associated with the acquisition of stem-like characteristics. Studies have shown the invasion potential of the CSC persistent across a variety of cancers in vivo and in vitro models[24].

Stem cell-based therapies exhibit profound therapeutic potential for treating cancer. Among the various types of stem cells, Mesenchymal stem cells (MSCs) are the most frequently used cell type for regenerative medicine. Also, Amniotic fluid-derived stem cells (AFSCs) have been shown to exhibit natural tropism towards cancer and are thus now being used as regenerative stem cell therapy[14,25].

The importance of CSCs came from their roles in tumor initiation, growth, and drug resistance. While targeting these cells is now becoming one of the potential strategies

for cancer treatment. Still, many underlying molecular mechanisms uninvestigated control and drive CSCs development. The regulation of CSC self-renewal is the critical link to understanding tumorigenesis. In this chapter, we briefly review the literature, emphasizing six crucial points that will allow us to understand the CSCs in a nutshell. These include CSC's characteristic features like cellular hierarchy, the role of CSCs in the tumor niche, biological regulation of the biological activity, abnormal metabolism, immune interactions, and drug resistance. In addition, we also give insight into potential therapeutic strategies to combat cancer by explicitly targeting CSCs. CSCs have gathered much attention over the last two decades. With the advancement of technology, much light has been shed on their molecular interactions and biological activity.

CSCs on the top of the cellular hierarchy

The concept of CSCs has been derived from the idea of stem cells, which govern their robust stemness state by core transcription factors OCT4, SOX2, and NANOG, where NANOG confers a stable undifferentiated embryonic stem cells (ESC) form[26, 27, 28]. These transcription factors play a critical role in major signaling pathways like the TGF-β, LIF/STAT3, Wnt/β-catenin, FGF/ERK, TGF/SMAD, and PKC[29] also activate ESC-specific genes conferring the stem cell characteristics by inhibiting the differentiation genes. The differentiation genes are active during organogenesis while the stemness markers are diminished or inactivated [30]. A characteristic signature of CSCs is to overexpress these embryonic genes to retain their stemness and plasticity[31]. The plasticity of the stem cell enables them to transit between epithelial and mesenchymal states (EMT),

which enhances their ability to invade tissue, dissemination, and metastasis[32]. The CSCs also maintain a quiescent state, meaning they exist in the G0 stage of the cell cycle in a nondividing state temporarily or reversibly[33]. Flow cytometry identifies the CSCs using classical cell surface markers like CD34, CD44, and CD138. Aldehyde dehydrogenase activity (ALDH) could also be used for identifying CSCs using an enzymatic assay. These characteristics put the CSCs on top of the cellular hierarchy in a tree-like apex. They take control of the neoplastic systems by differentiating or dedifferentiating into heterogeneous progenitor cancer cell types that make up the bulk of the primary tumor[34]. Matsuda and his team showed that the CSCs in vitro remain autonomously balanced with stem-like cells and differentiated cells along with the endothelial cells. The differentiated supporting cells secrete factors that stabilize the CSC's properties and differentiation lineage[35]. CSCs as highly tumorigenic cells could raise other progenitors and differentiated cells, therefore, maintaining tumor heterogeneity. Many types of cells have been shown to be driven from CSCs, such as fibroblasts, endothelial cells, and cancer differentiated cells.

Rulers of tumour niche

Cancer is a multifactorial disease. The hallmarks of tumor development include accumulating mutations that lead to self-sufficient growth signals and insensitivity to antigrowth signals. In addition, sustaining angiogenesis and evading apoptosis enables cancer cells to invade tissue and metastasize in other parts of the body[36]. Cancer-associated fibroblasts, Mesenchymal stem cells, Inflammatory cells like f natural killer cells (NKs) and CD8+ T cells, tumor-associated macrophages (TAM), tumor-associated

neutrophils (TAN) are the different types of cells that are housed by the CSC niche. In the tumor microenvironment, CSCs have been shown to release extracellular vesicles that influence the surrounding niche. Cancer cells and stromal cells also release exosomes taken up by CSCs or adult stem cells, leading to alterations to their phenotype[37]. These cells produce factors that contribute to self-renewal, inducing angiogenesis, immune recruitment, and other stromal cells. These stromal cells secrete additional factors that promote tumor invasion and metastasis[38]. Based on the histological characterization and interactions with the noncancerous cells present in the tumor ecosystem, the tumor microenvironment (TME) in solid tumors is divided into discrete compartments such as the perivascular region, hypoxic region, and the immune niche. Collectively these generate a dynamic self-sustaining tumor ecosystem[39-41]. Based on these special niches they attain, the CSCs reside, they display different transcriptional and epigenetic signatures. The perivascular region hosts the interaction between the endothelial cells (ECs) and the extracellular matrix (ECM) components, which is found more broadly in areas of metastatic growth and solid tumors, including melanoma, skin papilloma, and breast cancer. The ECS regulates the Notch, sonic hedgehog, and nitric oxide signaling that promotes the stemness of the CSCs. This region is an essential part of the tumor niche as it provides supportive niche and growth cues for the CSCs and increased vascularization. CSCs that reside on the hypoxic acidic and necrotic chambers are aggressive. Hypoxic stress due to oxygen deprivation is often accompanied by nutrient restriction and acidic stress[42]. Studies have shown that CSCs can survive and thrive in these nutrient-deprived regions [43]. This

microenvironment condition promotes the stemness and phenotype of quiescence and migration[44]. The consequence of hypoxia is majorly regulated by hypoxia-inducible factors (HIFs) that maintain pathways and confer maintenance of the hypoxic niche, promote immune escape, and trigger paracrine signaling, which confers vascularization. The immune niche hosts different profiles of immune cells across different tumor types. Tumor initiation depends immensely on the cancer cells' ability to avoid immune attacks. CSCs are immunosuppressive and thus are the main mechanics of tumorigenesis, and they can remodel immune response within the tumor microenvironment to evade death by immune cells[45]. Studies have found that the CSCs secret many immunosuppressive molecules such as TGF-β and IL4 that trigger antitumor response while secreting molecules like periostin (POSTN). The CSCs recruit M2 macrophages and interact with the macrophages physically via ligand-receptor binding of the CD90-CD11b and EphA4-Ephrin[46, 47, 48]. Tumor architecture is complex and includes different types of cells. Both cancer cells and no-cancer cells interact with each other in the TME. This interaction is shown to have essential roles in cancer progression and affect tumor characteristics such as invasion, metastasis, and drug resistance. These interactions within the TME seemingly make the CSCs rulers of the tumor niche[49, 50].

Regulation of Biological activity of CSCs

The mechanisms underlying the biology of tumor dormancy and their reactivation to start metastases can be explained through the biological activity of CSC. The underlying molecular mechanism to understand the biological activity of CSCs is

governed by a complex array of transcription factors, intracellular signaling pathways, and extracellular factors. The transcription factors OCT4, SOX2, NANOG, KLF4, NANOG, and MYC, provide the characteristics of stem cell-like features, including in vitro sphere formation assay [51- 54]. Wnt, Notch, Hedgehog (Hh), TGF-β, JAK/STAT3, and NF-κB pathways in CSCs are abnormally activated and are known as the self-renewal pathways. These pathways also contribute to the development and tissue homeostasis. Wnt signaling plays an important role in the self-renewal, dedifferentiation, apoptosis inhibition, and metastasis of CSC[55]. This pathway mediates biological processes through a canonical or non-canonical pathway, depending on the involvement of β-catenin in signal transduction[56]. The β-catenin is the core component of the cadherin protein complex. The stabilization of β-catenin is essential for the activation of the Wnt/β-catenin signaling[57]. Through this signaling pathway, CSCs mediate metastasis[58]. The nuclear factor-κB (NF-κB) pathway has an essential connection regulating inflammation, self-renewal, or maintenance and metastasis of CSCs[59]. CD44, TNFRSF19, Bmi-1, FOXP3, and SD-F1 proteins and microRNAs, miR-221, and miR-222, directly regulate the NF-κB pathway[60]. Also, this pathway is indirectly affected by some proteins like PGE2, GIT-1, CCR7, TGF-β, and miR-491 via the ERK and MAPK pathways[61]. The Notch signaling pathway is active on the CSCs and has been reported to promote cell survival, self-renewal, and metastasis and inhibit apoptosis[62]. The Notch signaling pathway consists of the Notch receptor, Notch ligand (DSL protein), CSL (CBF-1, suppressor of hairless, Lag), DNA-binding protein, other effectors, and Notch regulatory molecules. The expression of the Notch ligands and receptors varies across

different subtypes. For this reason, Notch can function both as an oncogene and a suppressive gene[63]. The PI3K/AKT/mTOR signaling pathway is considered a master regulator for cancer. It has been linked to promoting cell survival, maintenance of stemness, tumorigenicity, migration, and invasion in various types of CSCs[64, 65]. The Phosphatidylinositol-3-kinase (PI3K) is an intracellular phosphatidylinositol kinase that regulates the survival of the CSC residing in the perivascular region[66, 67.] The AKT is a serine/threonine kinase having three isoforms, AKT1, AKT2, and AKT3. The AKTs are effectors of PI3K and are directly activated in response to the PI3K [68, 69]. The mammalian target of rapamycin (mTOR) complex is a conserved serine/threonine kinase that is one of the key downstream targets of AKT. The mTOR binds with other proteins and serves as the key component of two protein complexes called the mTORC1 and mTORC2. The mTORC1 consists of subunits mTOR, raptor, mLST8, and two negative regulators, PRAS40 and DEPTOR. On the other hand, the mTORC2 comprises mTOR, RICTOR, MLST8, and mSIN1. The mTORC2 activates AKT by phosphorylating AKT at serine residue 473[70, 71]. The transforming growth factor‐β (TGF‐β) are secreted inflammatory cytokines that are involved in cellular processes associated with the organism and embryo development, including cell proliferation, differentiation, apoptosis, and homeostasis[72, 73]. TGF‐β1, TGF‐β2, and TGF‐β3 are the three subtypes, and they function by two transmembrane serine‐threonine kinase receptors, TGFβR1 and TGFβR2. The TGF-β ligand binds to the TGFβR2, then recruits the TGFβR1 and then phosphorylates it[74, 75]. The phosphorylated TGFβR1 then phosphorylates receptor-regulated SMADs (R- SMADs), which then binds to the

common pathway SMAD (co- SMAD)[76]. The R- SMAD/co- SMAD complex accumulates in the nucleus and acts as a transcription factor to regulate the expression of the target genes. Peroxisome proliferator-activated receptors (PPARs) are a subset of multifunctional ligand-activated nuclear transcription factors closely related to energy metabolism, dedifferentiation, proliferation, apoptosis, and inflammatory reactions. Besides, these PAARs also play an important role in the epithelial-mesenchymal transition (EMT) process in CSC initiation and the regulation of CSC functions[77]. Also, the CXCR4/CXCL12 signaling axis promotes metastasis and invasion across a wide variety of solid tumors. The expression of the CXCR4 defines pro-metastatic subpopulation, while the expression of CXCL12 defines higher risk regions for metastasis in breast cancer invasion[78]. Besides these major pathways, extracellular factors such as the vascular niches, hypoxia, tumor-associated macrophages, cancer-associated fibroblasts (CAFs), cancer-associated mesenchymal stem cells (CAMS), extracellular matrix, and exosomes also act as a regulator of CSCs[79].

Metabolic Plasticity

Metabolic plasticity is another hallmark of cancer cell adaptation that features increased metabolic activity, mitochondrial dysfunction, elevated peroxisome, oxidase, cyclooxygenases, lipoxygenases, thymidine phosphorylase, high oncogene activity, immune cell infiltration, and elevated cellular receptor signaling[80-82] (Figure 1). CSCs have the unique ability to switch between oxidative phosphorylation (OXPHOS) and glycolysis to produce energy (Figure: 1). The cancer cells use glycolysis, and CSCs rely heavily on OXPHOS as their primary energy source. When glucose is abundant in the

cellular system, the proliferating CSCs use aerobic glycolysis as a primary source of ATP production. Still, they change into a quiescent state during glucose and oxygen-deprived conditions and rely on OXPHOS for their biogenesis needs[83]. The unique metabolic flexibility of the CSCs helps them maintain homeostasis under low oxygen microenvironments, enabling them to promote tumor growth[84]. Metabolic switching from OXPHOS to glycolysis helps maintain stemness in CSCs by decreasing ROS levels in CD44, +CD24, and EPCAM expressing CSCs. Although studies have shown that CSCs mainly depend on oxidative metabolism, there is evidence that metabolic differences give rise to metabolic heterogeneity[85,86]. These differences include utilizing different energy sources, including glucose, lactate, pyruvate, hydroxybutyrate, acetate, glutamate, and fatty acids used by different subcellular compartments involving a range of cells. CSCs exhibit different metabolic phenotypes across different tumor types and among the subclones within the tumors. The glycolytic phenotype of CSCs shows high glucose consumption, lactate synthesis, ATP production, and the high expression of oncogenic MYC, which is a driver for stemness and glycolytic flux. MYC/PGC-1 has been shown to determine the metabolic phenotype and plasticity of pancreatic CSCs[87]. Different signaling contexts and oncogenic mutations within cancer cells confer metabolic phenotypes in CSCs, and these involve signaling pathways such as Notch, Wnt/β-catenin, PI3K/AKT, PTEN, NF-kB, KRAS, HIF, TP53. In most cancer cells, glucose uptake is significantly elevated, and oxidative phosphorylation in mitochondria is often decreased compared to normal cells. Mounting evidence indicates that hypoxia represents one of the essential features of the CSC niche[88]. The rapidly

growing mass often outpaces the local blood supply in solid tumors, thus generating hypoxic microenvironments. Besides, the dysfunctional biology of tumor vasculature delivers an aberrant blood flux, which lowers the oxygen availability in the tumor mass. It should be mentioned that although oxygen has a higher diffusion rate compared with glucose, the solubility of the oxygen is lower than that of glucose, which explains why glucose-based metabolism takes over in cancer contexts. Recently, a new population of CSCs has been isolated and named energetic CSCs (e-CSCs). They have more glycolytic, have higher mitochondrial mass, and showed significantly elevated oxidative metabolism and strictly depend on oxidative mitochondrial metabolism[89]. High mitochondrial biogenesis or metabolism are distinguishing features of CSCs (CSCs) that rule tumor initiation, metastatic dissemination, and therapy resistance in the CSCs Targeting mitochondrial metabolism may be a novel way to eliminate CSCs by blocking ETC complexes with compounds[90]. One of the ways to target CSCs is by treatment with Dodecyl-TPP that inhibits OXPHOS and activates glycolysis which promotes metabolic inflexibility in CSCs by depleting energy. This weakened metabolic state of CSCs makes them susceptible to inhibitors like vitamin C, berberine, doxycycline, niclosamide, 2-deoxy-glucose[91]. Another study reported Doxycycline, Azithromycin, and Vitamin C (DAV) could be used as a combination therapy by orchestrating functional energy depletion via inhibiting mitochondrial protein translation[92]. Also, e-CSCs can be successfully targeted with OXPHOS inhibitor, Diphenyleneiodonium (DPI), and CDK4/6 inhibitor (ribocilib)[89]. The CSCs elicit ROS-mediated cytotoxicity in bulk tumors by inducing oxidative stress. REDOX in CSCs contributes to plasticity. Recent studies have

shown that modulation of redox potential through co-inhibition of glycolysis and nuclear factor erythroid 2-related factor 3 (NRF-2)-mediated antioxidant responses are taken to disrupt the state equilibrium in CSCs in breast cancer, which leads to terminal differentiation and apoptosis[93]. Metformin, an inhibitor of OXPHOS complex I, has demonstrated anti-tumoral activity by reducing mammosphere formation, delaying in vivo tumor growth, and inducing apoptosis in pancreatic CSCs unable to switch to glycolysis[94].

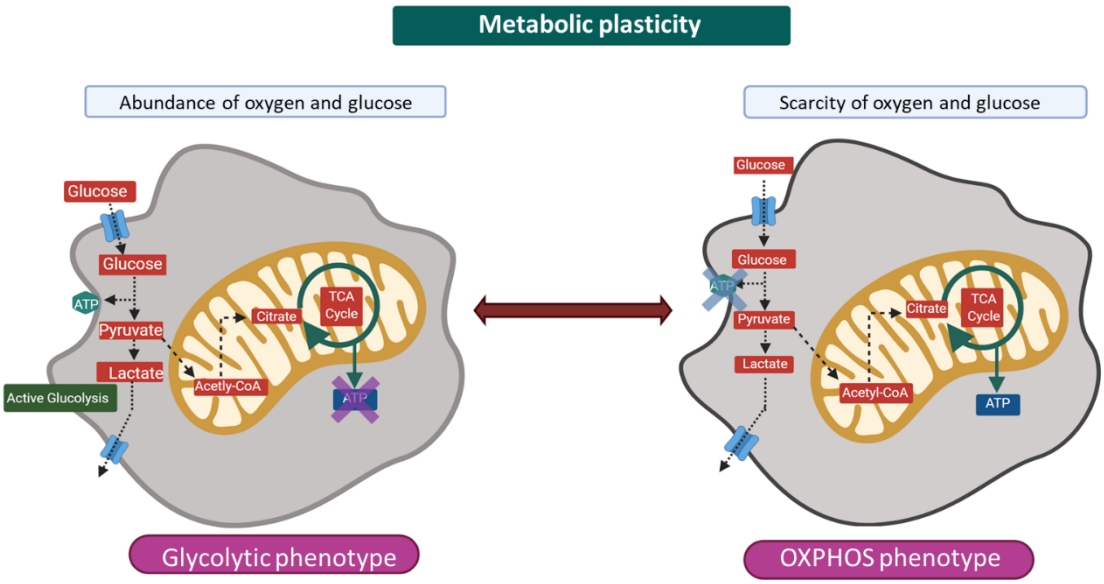

Figure 1: Schematic diagram shows the metabolic plasticity of CSC upon abundance or scarcity of Oxygen and Glucose

Circumventing immune response

Immunosurveillance is an essential tool for eliminating cancerous cells by immune cells that recognize cancer cells in the early stages before forming tumors (Figure 2). For

transformed cells to form tumors, they have to overcome immunosurveillance by developing immune escape mechanisms[95, 96]. In biological systems, immune cells act as early defenders against cancer. CSCs have gained the ability to evade immune destruction and foster the establishment of an immunosuppressive tumor microenvironment[97, 98]. CSCs have achieved this ability by the establishment of intricate interactions with and recruitment of a broad range of immune cells, including myeloid-derived suppressor cells (MDSCs), regulatory T cells (Tregs), tumor-associated macrophages (TAMs), and T helper (Th) cells in the TME[99,100]. Modifying the immunogenicity of cancer cells is another way to escape immune responses. The changes in the antigenicity of cancer cells lead to the dominance of the subpopulation and result in immunodominance CSCs in the tumor niche (Figure: 2). From this point, recent reports suggest that the acquiring of immune escape mechanisms in CSCs are responsible for the initiation of tumorigenicity. Expression of the major histocompatibility complex (MHC) is crucial for the immune detection of malignant cells by presenting tumor-specific antigens. Cancer cells that lose or down expressed MHC expression results in defective antigen presentation and make cells escape from immune responses by tumor-specific T cells. Thereby, the down-expressing of MHC-I molecules in CSCs boost tumorigenicity and reduce immune reaction against tumor cells through CTL killing[101,102]. CD44 positive CSCs have been reported to be decreasing MHC-I expression in contrast to CD44 negative, which is considered non-CSCs. Melanoma CSCs also express lower levels of the MHC-I and inhibit T-cell activation. Similarly, low expression of MHC-1 was reported in putative CSCs of colorectal cancer

and glioblastoma[45, 103]. Finally, macrophages were shown to play vital roles in tumor growth and progression. In tumor microenvironments, macrophages display different phenotypes known as tumor-associated macrophages (TAMs). In contrast to activated macrophages phenotype M1, which has anti-inflammation and anti-cancer properties, TAMs have tumor-supportive and immune-suppressive phenotypes. Recently, it has been reported that TAMs could induce CSCs from non-stem cancer cells and could regulate cancer cells' behavior by inducing dormancy that has stem cell-like properties [50]. Moreover, the interaction between TAMs and CSCs could also promote metastasis and drug resistance via a wide range of secreted factors. The CSCs also secrete soluble factors like Galectin-3, GDF-15, IL-10, IL-13, PGE2, and TGFβ, or express immune checkpoint molecules with immunosuppressive functions, which have been observed across various tumor types. By secreting these molecules, CSCs can regulate the impairment of immune responses as well as regulate a pro-tumoral TIME. Moreover, CSCs release pro-inflammatory cytokines such as IL-6, IL-8, IL-10, and IL-1. These can contribute to maintaining an inflammatory and suppressive TME representing the "niche" sustaining cellular stemness[104-107]. Therapies that target the whole bulk of the tumor usually fail to eradicate cancer and prevent relapse, mainly because of repopulating the tumor by CSCs. New therapies strategies have emerged to prevent relapse and efficiently treat cancers by focusing on targeting CSCs. As part of these efforts, many studies use immune targeting therapies against CSCs and treatments that boost the immune system as part of these efforts. Many immunotherapies have been approved to treat numerous types of cancer[108]. A

growing body of evidence shows that some specific CSCs antigens are effective targets of immunotherapy, such as olfactory receptor family 7 subfamily c member 1 in colon cancer, IL-3Ra receptor and T cell immunoglobulin mucin-3 in leukemia, CD133 in pancreatic and liver cancers. These reports reveal that using antibodies against CSCs, and antigens eliminated CSCs and reduced tumorigenicity[109-111]. On the other hand, CSCs antigens could also be used to design smart and targeted therapies against CSCs. Antibody conjugated nanoparticles for CD133 showed improvement in the treatment response and eliminated CD133 positive liver CSCs[112]. while immunotoxin against CD133 decreased tumor volume in Glioma CSCs[113]. For breast cancers, the combination of immunotherapy against CD133 positive CSCs and other treatments achieved better effects[114]. Furthermore, natural killer (NK) cells have also targeted CSCs in several hematologic and solid cancers. As those tumor cells showed to express ligands for NK cells receptors[115-117]. Therapies using NK cells showed the great effect of cytotoxicity on CSCs, inhibiting tumor growth and longer survival effects[118,119]. Thus, CSCs could be targets of the NK cell cytotoxicity-based treatments[120,121]. Finally, chimeric antigen receptor-modified T (CART) cells have been used recently as another treatment strategy targeting CSCs. CART targets cancer cells by modifying t-cells to express a specific CSC antigen receptor. Several CSCs specific antigens have been analyzed as potential targets of CART therapies as CD44, CD133 and EpCAM[122-125]. CAR-T showed the ability to recognize CSCs leading to activation of T-cells against CSCs and eliminating xenograft tumors *in vivo*[123].

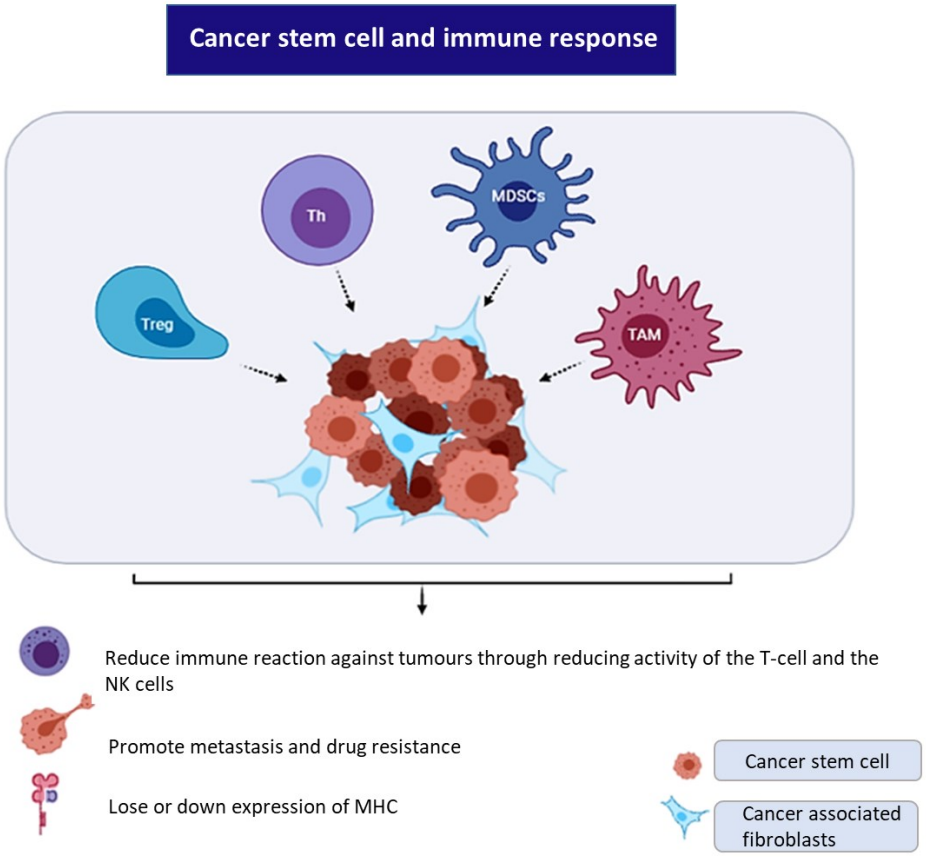

Figure 2: Interaction between cancer stem cells and immune cells in the tumor microenvironment. The interaction led to escaping from immune response through mechanisms such as down expression of MHC and reducing the activity of tumor eliminating cells (T-cells and NK cells). The interaction promotes metastasis and drug resistance of cancer cells

Focusing on CSC marker

The complex structure of tumors maintained by CSCs is thought to have a pivotal role in chemotherapy resistance characteristics. Recently many researchers tried to combine conventional drugs with CSC-targeting treatments to eradicate cancer and prevent relapse or metastasis. The CSCs have been identified and isolated based on

the expression of specific surface markers in many types of solid cancers. The most common markers include CD24, CD44, CD133, and ALDH1. Many reports suggest using combinations from more than one marker to identify or isolate CSCs since one marker is usually not efficient. In this chapter, we will focus on CD44 and CD133 based treatments as examples of marker-based therapies. CD44 is an adhesion receptor binding to hyaluronic acid (HA). CD44 has first been identified as a marker for breast CSCs, which are described as CD44+CD24− cells. CD44 has been suggested as a CSC marker in various solid tumors such as pancreatic, liver, gastric, head and neck, glioma, prostate, and ovarian. Monoclonal antibodies, aptamers, and nanoparticles have been used to target CD44 positive CSCs. Conjected HA with toxins and cytotoxic drugs help to precise targeting of CSCs at the same time help to improve the pharmacokinetic characterizations of those agents[126, 67]. Aires et al. showed that the HA nanoparticles drug delivery system specifically targets CSCs but not non-CSCs[127,128]. Finally, HA conjugated with doxorubicin and gemcitabine is reported to effectively inhibit the growth of triple-negative breast cancer in vivo models[129]. CD133 (prominin-1), a membrane glycoprotein, is suggested as CSCs markers in several solid tumor types such as glioblastoma, lung, colorectal, ovarian, pancreatic, breast, liver cancer. However, CSCs based on CD133 is still controversial since isolating CSCs depending on CD133 alone is insufficient, and CD133 may not be a unique marker of CSCs. Waldron showed that nanoparticles conjugated with CD133 aptamers could selectively eradicate CD133+ osteosarcoma CSCs in vitro and in vivo[130]. Finally, the identification and targeting of CSCs specific panels of markers could bring great significance in cancer

treatments in combination with modern drug delivery systems. For acute myeloid leukemia CSCs, the CD33 has been a significant marker[131]. It is a transmembrane protein that belongs to the sialic acid-binding sialoadhesin receptor (Siglec) family, which gets activated by cross-linking or ligand-binding. Activation of CD33 Leads to the phosphorylation f tyrosine of the intercellular inhibitory signaling motifs, recruitment and activation of SH2-containing phosphatases Shp-1 or Shp-2, and endocytosis of the CD33-ligand complex. CD33 has been targeted in numerous ways for AML. In a recent study, CD33+, chemo-resistant xeno-grafts were targeted using CAR-CIK cells, which had been specially genetically engineered using a specialized transposon system. These cells are derived from the Genetic engineering of T cells with chimeric antigen receptors1[27, 128].

CSCs and therapy resistance

CSCs resistance is determined by DNA repair capability. CSCs have the power to evade treatment like therapy or radiation therapy that contribute to the morbidity and mortality rate (Figure: 3). The drug resistance happens due to intrinsic or non-inheritable mechanisms which involve independent tumor factors that impede the delivery of active drugs and intratumor epigenetic factors that confer multiple mechanisms of chemoresistance (MOC)[132]. CSCs are innately resistant to therapy through their relative quiescence, their enhanced capacity for DNA repair, and ABC transporter expression (Figure 3).

Quiescent state

The quiescent state is considered part of stem cell and tissue maintenance, permitting stem cells to act as a cellular reserve allowing cell populations to be maintained and regenerated after injury. In this state, cells do not seem to be actively dividing. It is thought that therapy typically targets quickly dividing cells. Most cancer cells are eliminated; however, quiescent CSCs stay and act as reservoir cells, later cancer recurrence. Considered an essential characteristic of CSCs, quiescent cancer cells are incontestable in each solid and blood cancer wherever therapy resistance is present. Recent findings showed that CSCs are quiescent within the resting stage of the cell cycle and proof against therapy since those medication targets proliferating cells[133]. The upregulation of DNA repair proteins in CSCs correlates with speedy DNA repair, which additionally participates in drug and radiation resistance[134,135]. The quiescent

state of CSCs protects these cells from antiproliferative agents and is, therefore, a vital issue of CSC-related resistance to standard medical care.

Drug efflux

ATP-binding cassette (ABC) transporters bind to and hydrolyze a pair of ATP molecules and use the binding and reaction energy to either efflux specific compounds across the membrane or to flip them from the inner to the outer side of the membranes (Figure 1) [136-138]. CSCs express drug transporters are rendering them resistant to several therapeutic agents. Therefore, strategies to target these cells are needed. The ABC transporters are reportable to be overexpressed in CSC that use drug efflux pumps for repelling lipophilic chemotherapeutic agents like doxorubicin from cells[139]. Among the family of ABC transporters, ABCB1 and ABCG2 are proved to confer drug resistance. ABC transport inhibitors may well be re-invented as 'CSC sensitizers' targeting the foremost vital cells within the tumor. ABC inhibitors will not reduce tumor burden directly, and their efficiency could be monetized with alternative methods, such as the frequency of relapse or the time to relapse. It will be necessary to develop a panel of ABC transporters inhibitors in the future, mainly to ABCG2, the most crucial transporter for stem cells. Although fumitremorgin C (FTC) and Ko143 are specific ABCG2 inhibitors [140], FTC is toxic to cells and mice. A screen for ABCG2 inhibitors has yielded a collection of the latest candidates, several of which are amenable to structural modification to spot a potent antagonist. Peptides mimicking TM domains of ABC transporters have been verified to be selective and specific inhibitors and will, in essence, be designed for any transporter[141].

Increased DNA damage responses (DDR)

Accumulated evidence indicates that CSC populations are resistant to therapy through increased DNA repair response[136-138]. This property of activation or increased DNA response causes resistance to any exogenous DNA damage that leads to the failure of cancer therapy [139-141]. Although DDR is critical to the maintenance of genome stability in normal cases, increased DNA repair can reduce the efficacy of DNA damaging agents in treating cancers. DNA damaging agents used for cancer therapy can induce various DNA lesions, such as covalent crosslinks between DNA bases, base alkylation, DNA single-strand breaks (SSB) and double-strand breaks (DSB). DNA damage response is a hierarchical process performed through a sequence of steps. The DNA lesions are distinguished by sensor proteins that identify chromatin alterations that result from the DNA damage. Transducers are then brought into action to deliver the damage signal to downstream effectors. It is this relay system from transducers to effectors that permits a single DNA lesion to modulate numerous pathways. The transducers may also be involved within the assembly of DNA-repair complexes at the sites of DNA damage[142]. Following sensing of a DNA double-strand break (DSB), ATM protein is activated, and a portion of the nuclear ATM binds to DSB sites[143]. DDR and the expression of various repair proteins are also found to be highly up-regulated in tumour-initiating cells isolated from mouse mammary gland tumours, indicating an elevated DDR in these CSCs[144]. A significant increase in the expression of DNA repair-related genes, such as BRCA1 and RAD51, have also been observed in pancreatic CSCs

compared with bulk cells. These spheroid cells also repair DNA breaks more efficiently than bulk cells after treatment with gemcitabine[145-147].

Nucleotide excision repair

Nucleotide Excision Repair (NER) is considered the most critical repair pathway in cancer, including CSCs. The NER can deal with a broad spectrum of DNA lesions developed from either endogenous or exogenous mediators. It removes DNA lesions such as crosslinks, photolesions, alkylation adducts, and bulky aromatic hydrocarbons. NER is a multistep pathway that removes the helix-distorting lesions using the above thirty proteins. The damaged DNA bases are recognized by RAD23B (UV excision repair protein) and XPC (xeroderma pigmentosum complementation group C)154, whereas XPA (DNA repair protein complementing XP-A cells), RPA (replication protein A), RNA polymerase II transcription factor 11A and XPG excise the fragment of 27–30 nucleotides surrounding the damaged bases. XPA is well-thought-out to be a central coordinator of the NER, which stimulates lesion verification by TFIIH155, and binding to altered nucleotides in ssDNA in addition to interaction with almost all NER proteins156. NER removes several structurally unrelated DNA lesions by a multi-wise 'cut and patch'-type reaction. The global genome NER (GG-NER) avoids mutagenesis by probing the genome for helix-distorting lesions. At the same time, transcription-coupled NER (TC-NER) eliminates transcription-blocking lesions to permit unperturbed gene expression, thus preventing cell death. Consequently, defects in GG-NER result in cancer predisposition. Damage-induced phosphorylation72, poly (ADP-ribosylation)

(PARylation), sumoylation and ubiquitylation have been shown to regulate NER157-160.

Resistant to redox stress (ROX)

The ability to control cellular levels of ROS is one of the best-understood factors that regulate the biology of stem cells. At the same time, excess amounts of ROS limit the function of HSCs161. At typical physiologic altitudes, ROS are essential for the appropriate part of the stem and progenitor cells162, 163. Consequently, cautious regulation of ROS can play a programmatic role in stem cell quiescence and differentiation fate. On the other hand, redox regulation is considered critical for cancer recurrence through resistance to chemotherapy or radiotherapy. The CSCs possess this potential of redox regulation by controlling low ROS production levels and sifting ROS-dependent signaling pathways. The lower level of ROS maintained by CSCs through overexpression of antioxidant enzymes, which assist them in surviving from therapeutic agents.

BRCA DNA damage repair pathway

The BRCA (Breast Cancer) genes are part of a complex that repairs double-strand breaks in DNA for normal and disease. DNA cross-linking agents are an essential source of chromosome/DNA damage. Both BRCA1 and BRCA2 are essential genes for cellular development165, 169. It has been demonstrated that these genes are required for the maintenance of genome integrity and resistance to DNA damage168, 170. Moreover, without functional BRCA genes, cells are inefficient in repairing DNA damage by homologous recombination, which may cause apoptosis or cell transformation171-173.

The BRCA1 and BRCA2 work together as part of a complex that acts directly in double-strand break (DSB) repair. BRCA1 and BRCA2 defective cell lines exhibit similar sensitivities to DNA-damaging agents and show defects in DSB repair, which in turn show us the critical role of those genes165, 173. BRCA1 Likely plays an important role in the function and behavior of stem cells in a large subset of cancer. BRCA1 is frequently mutated in human cancers, which is associated with global chromosome instability and tumor formation174. Many chemotherapeutic agents exercise anti-cancer efforts by inducing DNA damage. To oppose DNA damage, the tumor cells, especially CSCs (CSCs), activate DNA damage repair pathway-related genes like BRCA.ts164, so this property is considered one of the most critical problems during therapy.

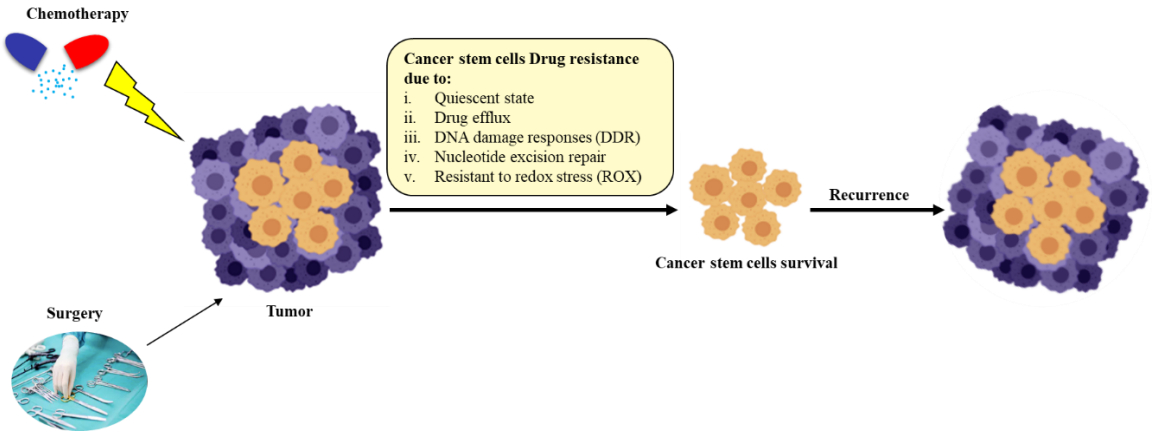

Figure 3: Schematic diagram representing the over all idea of CSC therapy resistance.

Conclusion

The alarming increase in cancer prevalence indicates the need for a proper understanding of the pathophysiology of cancer. Previously developed standard models for cancers indicated that all carcinogenic cells hold equal potential for malignancy, tumorigenicity, and metastasis. However, recent advances in oncology reveal that tumors are highly heterogeneous. The cells present in the cancer hold variable states of differentiation, which directly affects the gene expression, immune response, tumor metastasis, propagation potential, and reaction to therapy. Different arrays contribute to the characteristic nature of tumors, such as genetic and epigenetic clonal variation, metabolic shifts, and microenvironmental factors. Combinational treatment strategies depending on the location, the grade of the tumor, and stage of the disease include surgery, postoperative adjuvant radiation therapy or chemotherapy, hormonal therapy, nanoparticles-based hyperthermia, photodynamic photo-thermal or targeted therapy like immunotherapy or synthetic lethality. Patient-derived CSCs are hard to isolate, and the process is rather complicated and time-consuming. With the recent advancement of new technologies, it is possible to investigate different cellular mechanisms that allow us to understand the conversion process more lucidly, allowing us to design a more efficient drug delivery system to combat CSCs.

Reference

1. Bray, F., et al., (2018) Global cancer statistics 2018: GLOBOCAN estimates of incidence and mortality worldwide for 36 cancers in 185 countries. CA: a cancer journal for clinicians. 68(6): p. 394-424.

2. Ferlay, J., et al., (2019) Estimating the global cancer incidence and mortality in 2018: GLOBOCAN sources and methods. International journal of cancer. 144(8): p. 1941-1953.

3. Syriopoulou, E., et al., (2017) Estimating the impact of a cancer diagnosis on life expectancy by socio-economic group for a range of cancer types in England. British journal of cancer. 117(9): p. 1419-1426.

4. Schatton, T., N.Y. Frank, and M.H. Frank, (2009) Identification and targeting of cancer stem cells. Bioessays. 31(10): p. 1038-1049.

5. Quintana, E., et al., (2010) Phenotypic heterogeneity among tumorigenic melanoma cells from patients that is reversible and not hierarchically organized. Cancer cell. 18(5): p. 510-523.

6. Visvader, J.E. and G.J. Lindeman, (2012) Cancer stem cells: current status and evolving complexities. Cell stem cell. 10(6): p. 717-728.

7. Eppert, K., et al., (2011) Stem cell gene expression programs influence clinical outcome in human leukemia. Nature medicine. 17(9): p. 1086-1093.

8. Konrad, C.V., et al., (2017) The role of cancer stem cells in tumor heterogeneity and resistance to therapy. Canadian journal of physiology and pharmacology. 95(1): p. 1-15.

9. Makino, S., (1959) The role of tumor stem-cells in regrowth of the tumor following drastic applications. Acta-Unio Internationalis Contra Cancrum. 15: p. 196.

10. Makino, S., (1956) Further evidence favoring the concept of the stem cell in ascites tumors of rats. Annals of the New York Academy of Sciences. 63(5): p. 818-830.

11. Heppner, G.H., (1984) Tumor heterogeneity. Cancer research. 44(6): p. 2259-2265.

12. Hamburger, A.W. and S.E. Salmon, (1977) Primary bioassay of human tumor stem cells. Science. 197(4302): p. 461-463.

13. Bergsagel, D. and F. Valeriote, (1968) Growth characteristics of a mouse plasma cell tumor. Cancer Research. 28(11): p. 2187-2196.

14. Lapidot, T., et al., (1994) A cell initiating human acute myeloid leukaemia after transplantation into SCID mice. Nature. 367(6464): p. 645-648.

15. Bonnet, D. and J.E. Dick, (1997) Human acute myeloid leukemia is organized as a hierarchy that originates from a primitive hematopoietic cell. Nature medicine. 3(7): p. 730-737.

16. Zhang, M., et al., (2008) Identification of tumor-initiating cells in a p53-null mouse model of breast cancer. Cancer research. 68(12): p. 4674-4682.

17. Al-Hajj, M., et al., (2003) Prospective identification of tumorigenic breast cancer cells. Proceedings of the National Academy of Sciences. 100(7): p. 3983-3988.

18. Vaiopoulos, A.G., et al., (2012) Colorectal cancer stem cells. Stem cells. 30(3): p. 363-371.

19. Li, C., et al., (2007) Identification of pancreatic cancer stem cells. Cancer research. 67(3): p. 1030-1037.

20. Yamashita, T. and X.W. Wang, (2013) Cancer stem cells in the development of liver cancer. The Journal of clinical investigation. 123(5): p. 1911-1918.

21. Wang, J., Y. Ma, and M.K. Cooper, (2013) Cancer stem cells in glioma: challenges and opportunities. Translational cancer research. 2(5): p. 429.

22. Schatton, T., et al., (2008) Identification of cells initiating human melanomas. Nature. 451(7176): p. 345-349.

23. Abdullah, L.N. and E.K.-H. Chow, (2013) Mechanisms of chemoresistance in cancer stem cells. Clinical and translational medicine. 2(1): p. 3.

24. Chambers, I. and A. Smith, (2004) Self-renewal of teratocarcinoma and embryonic stem cells. Oncogene. 23(43): p. 7150-7160.

25. Niwa, H., (2007) How is pluripotency determined and maintained? Development. 134(4): p. 635-646.

26. Silva, J. and A. Smith, (2008) Capturing pluripotency. Cell. 132(4): p. 532-536.

27. Huang, G., et al., (2015) Molecular basis of embryonic stem cell self-renewal: from signaling pathways to pluripotency network. Cellular and molecular life sciences. 72(9): p. 1741-1757.

28. Dvash, T., et al., (2004) Temporal gene expression during differentiation of human embryonic stem cells and embryoid bodies. Human Reproduction. 19(12): p. 2875-2883.

29. Condiotti, R., W. Guo, and I. Ben-Porath, (2014) Evolving views of breast cancer stem cells and their differentiation states. Critical Reviews™ in Oncogenesis. 19(5).

30. Liu, S., et al., (2014) Breast cancer stem cells transition between epithelial and mesenchymal states reflective of their normal counterparts. Stem cell reports. 2(1): p. 78-91.

31. Chen, W., et al., (2016) Cancer stem cell quiescence and plasticity as major challenges in cancer therapy. Stem cells international. 2016.

32. Gasch, C., et al., (2017) Catching moving targets: cancer stem cell hierarchies, therapy-resistance & considerations for clinical intervention. Molecular Cancer. 16(1): p. 1-15.

33. Matsuda, S., et al., (2014) Cancer stem cells maintain a hierarchy of differentiation by creating their niche. International journal of cancer. 135(1): p. 27-36.

34. Hanahan, D. and R. Weinberg, (2000) The hallmarks of cancer. cell, 100. Transpl. Immunol. 5: p. 179-183.

35. Gilbertson, R.J. and J.N. Rich, (2007) Making a tumour's bed: glioblastoma stem cells and the vascular niche. Nature Reviews Cancer. 7(10): p. 733-736.

36. Plaks, V., N. Kong, and Z. Werb, (2015) The cancer stem cell niche: how essential is the niche in regulating stemness of tumor cells? Cell stem cell. 16(3): p. 225-238.

37. Zhang, C., et al., (2016) Hypoxia induces the breast cancer stem cell phenotype by HIF-dependent and ALKBH5-mediated m6A-demethylation of NANOG mRNA. Proceedings of the National Academy of Sciences. 113(14): p. E2047-E2056.

38. Prager, B.C., et al., (2019) Cancer stem cells: the architects of the tumor ecosystem. Cell Stem Cell. 24(1): p. 41-53.

39. Leong, L., (2007) 1: Diehn M, Cho RW, Lobo NA, Kalisky T, Dorie MJ, Kulp AN, Qian D, Lam JS, Ailles LE, Wong M, Joshua B, Kaplan MJ, Wapnir I, Dirbas FM, Somlo G, Garberoglio C, Paz B, Shen J, Lau SK, Quake SR, Brown JM, Weissman IL, Clarke MF. Association of reactive oxygen species levels and radioresistance in cancer stem cells. Nature. 2009 Apr 9; 458 (7239): 780-3. doi: 10.1038/nature07733. PubMed PMID: 19194462. Oncol. 14(11): p. 3168-73.

40. Bruttel, V.S. and J. Wischhusen, (2014) Cancer stem cell immunology: key to understanding tumorigenesis and tumor immune escape? Frontiers in immunology. 5: p. 360.

41. McWhorter, F.Y., C.T. Davis, and W.F. Liu, (2015) Physical and mechanical regulation of macrophage phenotype and function. Cellular and Molecular Life Sciences. 72(7): p. 1303-1316.

42. Lu, H., et al., (2014) A breast cancer stem cell niche supported by juxtacrine signalling from monocytes and macrophages. Nature cell biology. 16(11): p. 1105-1117.

43. Zhou, W., et al., (2015) Periostin secreted by glioblastoma stem cells recruits M2 tumour-associated macrophages and promotes malignant growth. Nature cell biology. 17(2): p. 170-182.

44. Malanchi, I., et al., (2012) Interactions between cancer stem cells and their niche govern metastatic colonization. Nature. 481(7379): p. 85-89.

45. Hassan, G. and M. Seno, (2020) Blood and Cancer: Cancer Stem Cells as Origin of Hematopoietic Cells in Solid Tumor Microenvironments. Cells. 9(5): p. 1293.

46. Matthes-Martin, S., et al., (2013) Stem cell transplantation after reduced-intensity conditioning for sickle cell disease. European journal of haematology. 90(4): p. 308-312.

47. Nichols, J. and A. Smith, (2009) Naive and primed pluripotent states. Cell stem cell. 4(6): p. 487-492.

48. Okita, K., T. Ichisaka, and S. Yamanaka, (2007) Generation of germline-competent induced pluripotent stem cells. nature. 448(7151): p. 313-317.

49. Takahashi, K., et al., (2007) Induction of pluripotent stem cells from adult human fibroblasts by defined factors. cell. 131(5): p. 861-872.

50. Logan, C.Y. and R. Nusse, (2004) The Wnt signaling pathway in development and disease. Annu. Rev. Cell Dev. Biol. 20: p. 781-810.

51. Katoh, M., (2017) Canonical and non-canonical WNT signaling in cancer stem cells and their niches: Cellular heterogeneity, omics reprogramming, targeted therapy and tumor plasticity. International journal of oncology. 51(5): p. 1357-1369.

52. Latres, E., D. Chiaur, and M. Pagano, (1999) The human F box protein β-Trcp associates with the Cul1/Skp1 complex and regulates the stability of β-catenin. Oncogene. 18(4): p. 849-854.

53. Jang, G.-B., et al., (2015) Blockade of Wnt/β-catenin signaling suppresses breast cancer metastasis by inhibiting CSC-like phenotype. Scientific reports. 5: p. 12465.

54. Rinkenbaugh, A.L. and A.S. Baldwin, (2016) The NF-κB pathway and cancer stem cells. Cells. 5(2): p. 16.

55. Li, B., et al., (2017) miR-221/222 promote cancer stem-like cell properties and tumor growth of breast cancer via targeting PTEN and sustained Akt/NF-κB/COX-2 activation. Chemico-Biological Interactions. 277: p. 33-42.

56. Richmond, A., (2002) NF-κB, chemokine gene transcription and tumour growth. Nature Reviews Immunology. 2(9): p. 664-674.

57. Stylianou, S., R.B. Clarke, and K. Brennan, (2006) Aberrant activation of notch signaling in human breast cancer. Cancer research. 66(3): p. 1517-1525.

58. Bray, S.J., (2006) Notch signalling: a simple pathway becomes complex. Nature reviews Molecular cell biology. 7(9): p. 678-689.

59. Chang, L., et al., (2013) Acquisition of epithelial–mesenchymal transition and cancer stem cell phenotypes is associated with activation of the PI3K/Akt/mTOR pathway in prostate cancer radioresistance. Cell death & disease. 4(10): p. e875-e875.

60. Oo, A.K.K., et al., (2018) Up-regulation of PI 3-kinases and the activation of PI3K-Akt signaling pathway in cancer stem-like cells through DNA hypomethylation mediated by the cancer microenvironment. 11(3): p. 653-663.

61. Vanhaesebroeck, B., et al., (2010) The emerging mechanisms of isoform-specific PI3K signalling. 11(5): p. 329-341.

62. Seno, M., et al. DNA Hypomethylation and overexpression of Class IB PI3K genes in the Oncogenic Conversion of iPSCs into CSCs. in CANCER SCIENCE. 2018. WILEY 111 RIVER ST, HOBOKEN 07030-5774, NJ USA.

63. Vergadi, E., et al., (2017) Akt signaling pathway in macrophage activation and M1/M2 polarization. 198(3): p. 1006-1014.

64. Polivka Jr, J., F.J.P. Janku, and therapeutics, (2014) Molecular targets for cancer therapy in the PI3K/AKT/mTOR pathway. 142(2): p. 164-175.

65. Knowles, M.A., et al., (2009) Phosphatidylinositol 3-kinase (PI3K) pathway activation in bladder cancer. Cancer and Metastasis Reviews. 28(3-4): p. 305-316.

66. Loewith, R., et al., (2002) Two TOR complexes, only one of which is rapamycin sensitive, have distinct roles in cell growth control. 10(3): p. 457-468.

67. Romero-Gallo, J., et al., (2005) Inactivation of TGF-β signaling in hepatocytes results in an increased proliferative response after partial hepatectomy. 24(18): p. 3028-3041.

68. Knabbe, C., et al., (1987) Evidence that transforming growth factor-β is a hormonally regulated negative growth factor in human breast cancer cells. 48(3): p. 417-428.

69. Liu, S., et al., (2016) Regulation of the TGF-β pathway by deubiquitinases in cancer. 76: p. 135-145.

70. Sakaki-Yumoto, M., Y. Katsuno, and R.J.B.e.B.A.-G.S. Derynck, (2013) TGF-β family signaling in stem cells. 1830(2): p. 2280-2296.

71. Brown, J.A., et al., (2017) TGF-β-induced quiescence mediates chemoresistance of tumor-propagating cells in squamous cell carcinoma. Cell stem cell. 21(5): p. 650-664. e8.

72. Issemann, I. and S. Green, (1990) Activation of a member of the steroid hormone receptor superfamily by peroxisome proliferators. Nature. 347(6294): p. 645-650.

73. Calinescu, A.-A., et al., (2017) Survival and Proliferation of Neural Progenitor–Derived Glioblastomas Under Hypoxic Stress is Controlled by a CXCL12/CXCR4 Autocrine-Positive Feedback Mechanism. Clinical Cancer Research. 23(5): p. 1250-1262.

74. Xu, J., K. Liao, and W.J.S.c.i. Zhou, (2018) Exosomes regulate the transformation of cancer cells in cancer stem cell homeostasis. 2018.

75. Vander Heiden, M.G., L.C. Cantley, and C.B.J.s. Thompson, (2009) Understanding the Warburg effect: the metabolic requirements of cell proliferation. 324(5930): p. 1029-1033.

76. Kamphorst, J.J., et al., (2015) Human pancreatic cancer tumors are nutrient poor and tumor cells actively scavenge extracellular protein. 75(3): p. 544-553.

77. Hensley, C.T., et al., (2016) Metabolic heterogeneity in human lung tumors. 164(4): p. 681-694.

78. Jose, C., N. Bellance, and R. Rossignol, (2011) Choosing between glycolysis and oxidative phosphorylation: a tumor's dilemma? Biochimica et Biophysica Acta (BBA)-Bioenergetics. 1807(6): p. 552-561.

79. Jia, D., et al., (2019) Elucidating cancer metabolic plasticity by coupling gene regulation with metabolic pathways. Proceedings of the National Academy of Sciences. 116(9): p. 3909-3918.

80. Sancho, P., D. Barneda, and C.J.B.j.o.c. Heeschen, (2016) Hallmarks of cancer stem cell metabolism. 114(12): p. 1305-1312.

81. Cliff, T.S., S.J.C.o.i.g. Dalton, and development, (2017) Metabolic switching and cell fate decisions: implications for pluripotency, reprogramming and development. 46: p. 44-49.

82. Scarpulla, R.C.J.B.e.b.a.-m.c.r., (2011) Metabolic control of mitochondrial biogenesis through the PGC-1 family regulatory network. 1813(7): p. 1269-1278.

83. Najafi, M., et al., (2020) Hypoxia in solid tumors: a key promoter of cancer stem cell (CSC) resistance. 146(1): p. 19-31.

84. Fiorillo, M., F. Sotgia, and M.P. Lisanti, (2019) “Energetic” cancer stem cells (e-CSCs): a new hyper-metabolic and proliferative tumor cell phenotype, driven by mitochondrial energy. Frontiers in oncology. 8: p. 677.

85. Aminzadeh-Gohari, S., et al. From old to new—Repurposing drugs to target mitochondrial energy metabolism in cancer. in Seminars in cell & developmental biology. 2020. Elsevier.

86. De Francesco, E.M., et al., (2019) Dodecyl-TPP Targets Mitochondria and Potently Eradicates Cancer Stem Cells (CSCs): Synergy With FDA-Approved Drugs and Natural Compounds (Vitamin C and Berberine). Frontiers in oncology. 9: p. 615.

87. Fiorillo, M., et al., (2019) Doxycycline, Azithromycin and Vitamin C (DAV): A potent combination therapy for targeting mitochondria and eradicating cancer stem cells (CSCs). Aging (Albany NY). 11(8): p. 2202.

88. Luo, M., et al., (2018) Targeting breast cancer stem cell state equilibrium through modulation of redox signaling. 28(1): p. 69-86. e6.

89. Malinowski, B., N. Musiała, and M.J.C. Wiciński, (2020) Metformin's Modulatory Effects on miRNAs Function in Cancer Stem Cells—A Systematic Review. 9(6): p. 1401.

90. Kim, R., Cancer immunoediting: from immune surveillance to immune escape, in Cancer Immunotherapy. 2007, Elsevier. p. 9-27.

91. Stewart, T. and S.J.O. Abrams, (2008) How tumours escape mass destruction. 27(45): p. 5894-5903.

92. Vahidian, F., et al., (2019) Interactions between cancer stem cells, immune system and some environmental components: friends or foes? 208: p. 19-29.

93. Schatton, T. and M.H.J.A.o.t.N.Y.A.o.S. Frank, (2009) Antitumor immunity and cancer stem cells. 1176: p. 154.

94. Lorenzo-Sanz, L. and P.J.C.M. Muñoz, (2019) Tumor-Infiltrating Immunosuppressive Cells in Cancer-Cell Plasticity, Tumor Progression and Therapy Response. 12(2-3): p. 119-132.

95. Rezalotfi, A., et al., (2019) Gastric cancer stem cells effect on Th17/Treg balance; a bench to beside perspective. 9: p. 226.

96. Iorgulescu, J.B., et al., (2018) Acquired mechanisms of immune escape in cancer following immunotherapy. Genome medicine. 10(1): p. 1-4.

97. Triaca, V., et al., (2019) Cancer stem cells-driven tumor growth and immune escape: the Janus face of neurotrophins. 11(23): p. 11770.

98. Sultan, M., et al., (2017) Hide-and-seek: the interplay between cancer stem cells and the immune system. 38(2): p. 107-118.

99. Crucitti, A., et al., (2015) Laparoscopic surgery for colorectal cancer is not associated with an increase in the circulating levels of several inflammation-related factors. 16(5): p. 671-677.

100. Ravindran, S., S. Rasool, and C.J.C.M. Maccalli, (2019) The cross talk between cancer stem cells/cancer initiating cells and tumor microenvironment: The missing piece of the puzzle for the efficient targeting of these cells with immunotherapy. 12(2-3): p. 133-148.

101. Rasool, S., et al., Cancer Stem Cells: The Players of Immune Evasion from Immunotherapy, in Cancer Stem Cell Resistance to Targeted Therapy. 2019, Springer. p. 223-249.

102. Wischhusen, J., I. Melero, and W.H. Fridman, (2020) Growth/Differentiation Factor-15 (GDF-15): From Biomarker to Novel Targetable Immune Checkpoint. Frontiers in Immunology. 11.

103. Codd, A.S., et al., (2018) Cancer stem cells as targets for immunotherapy. Immunology. 153(3): p. 304-314.

104. Morita, R., et al., (2016) Olfactory receptor family 7 subfamily C member 1 is a novel marker of colon cancer–initiating cells and is a potent target of immunotherapy. 22(13): p. 3298-3309.

105. Kikushige, Y., et al., (2010) TIM-3 is a promising target to selectively kill acute myeloid leukemia stem cells. Cell stem cell. 7(6): p. 708-717.

106. Huang, J., et al., (2013) Cytokine-induced killer (CIK) cells bound with anti-CD3/anti-CD133 bispecific antibodies target CD133high cancer stem cells in vitro and in vivo. Clinical immunology. 149(1): p. 156-168.

107. Jin, C., et al., (2014) Paclitaxel-loaded nanoparticles decorated with anti-CD133 antibody: a targeted therapy for liver cancer stem cells. Journal of nanoparticle research. 16(1): p. 2157.

108. Vora, P., et al., (2020) The Rational Development of CD133-Targeting Immunotherapies for Glioblastoma.

109. Klapdor, R., et al., (2017) Improved Killing of Ovarian Cancer Stem Cells by Combining a Novel Chimeric Antigen Receptor–Based Immunotherapy and Chemotherapy. 28(10): p. 886-896.

110. Kashii, Y., et al., (1999) Constitutive expression and role of the TNF family ligands in apoptotic killing of tumor cells by human NK cells. 163(10): p. 5358-5366.

111. Sakamoto, N., et al., (2015) Phase I clinical trial of autologous NK cell therapy using novel expansion method in patients with advanced digestive cancer. 13(1): p. 277.

112. Castriconi, R., et al., (2009) NK cells recognize and kill human glioblastoma cells with stem cell-like properties. The Journal of Immunology. 182(6): p. 3530-3539.

113. de Andrade, L.F., et al., (2018) Antibody-mediated inhibition of MICA and MICB shedding promotes NK cell–driven tumor immunity. Science. 359(6383): p. 1537-1542.

114. Ames, E., et al., (2015) Enhanced targeting of stem-like solid tumor cells with radiation and natural killer cells. Oncoimmunology. 4(9): p. e1036212.

115. Tseng, H.-C., et al., (2010) Increased lysis of stem cells but not their differentiated cells by natural killer cells; de-differentiation or reprogramming activates NK cells. 5(7): p. e11590.

116. Tallerico, R., et al., (2013) Human NK cells selective targeting of colon cancer–initiating cells: A role for natural cytotoxicity receptors and MHC class I molecules. 190(5): p. 2381-2390.

117. Wang, Y., et al., (2018) CD133-directed CAR T cells for advanced metastasis malignancies: a phase I trial. 7(7): p. e1440169.

118. Deng, Z., et al., (2015) Adoptive T-cell therapy of prostate cancer targeting the cancer stem cell antigen EpCAM. BMC immunology. 16(1): p. 1-9.

119. Choi, B.D., et al., (2018) Chimeric antigen receptor T-cell immunotherapy for glioblastoma: practical insights for neurosurgeons. Neurosurgical focus. 44(6): p. E13.

120. Casucci, M., et al., (2013) CD44v6-targeted T cells mediate potent antitumor effects against acute myeloid leukemia and multiple myeloma. Blood. 122(20): p. 3461-3472.

121. Ranji, P., et al., (2016) Targeting cancer stem cell-specific markers and/or associated signaling pathways for overcoming cancer drug resistance. 37(10): p. 13059-13075.

122. Aires, A., et al., (2016) Multifunctionalized iron oxide nanoparticles for selective drug delivery to CD44-positive cancer cells. 27(6): p. 065103.

123. Chen, B., R.J. Miller, and P.K.J.J.o.b.n. Dhal, (2014) Hyaluronic acid-based drug conjugates: state-of-the-art and perspectives. 10(1): p. 4-16.

124. Vogus, D.R., et al., (2017) A hyaluronic acid conjugate engineered to synergistically and sequentially deliver gemcitabine and doxorubicin to treat triple negative breast cancer. 267: p. 191-202.

125. Waldron, N.N., et al., (2014) A bispecific EpCAM/CD133-targeted toxin is effective against carcinoma. 9(3): p. 239-249.

126. Gottesman, M.M., T. Fojo, and S.E. Bates, (2002) Multidrug resistance in cancer: role of ATP–dependent transporters. Nature Reviews Cancer. 2(1): p. 48-58.

127. Snyder, V., et al., (2018) Cancer stem cell metabolism and potential therapeutic targets. 8: p. 203.

128. Colak, S. and J.P. Medema, (2014) Cancer stem cells–important players in tumor therapy resistance. The FEBS journal. 281(21): p. 4779-4791.

129. Somasagara, R.R., et al., (2017) RAD6 promotes DNA repair and stem cell signaling in ovarian cancer and is a promising therapeutic target to prevent and treat acquired chemoresistance. 36(48): p. 6680-6690.

130. Higgins, C.F.J.A.r.o.c.b., (1992) ABC transporters: from microorganisms to man. 8(1): p. 67-113.

131. Childs, S., (1994) The MDR superfamily of genes and its biological implications. Important Adv Oncol.

132. Dean, M. and R. Allikmets, (1995) Evolution of ATP-binding cassette transporter genes. Current opinion in genetics & development. 5(6): p. 779-785.

133. Doyle, L.A. and D.D. Ross, (2003) Multidrug resistance mediated by the breast cancer resistance protein BCRP (ABCG2). Oncogene. 22(47): p. 7340-7358.

134. Rabindran, S.K., et al., (2000) Fumitremorgin C reverses multidrug resistance in cells transfected with the breast cancer resistance protein. 60(1): p. 47-50.

135. Tarasova, N.I., et al., (2005) Transmembrane inhibitors of P-glycoprotein, an ABC transporter. 48(11): p. 3768-3775.

136. Bao, S., et al., (2006) Glioma stem cells promote radioresistance by preferential activation of the DNA damage response. 444(7120): p. 756-760.

137. Maugeri-Saccà, M., M. Bartucci, and R.J.M.c.t. De Maria, (2012) DNA damage repair pathways in cancer stem cells. 11(8): p. 1627-1636.

138. Abad, E., D. Graifer, and A.J.C.L. Lyakhovich, (2020) DNA damage response and resistance of cancer stem cells. 474: p. 106-117.

139. Suman, S., et al., (2020) Heavy ion space radiation triggers ongoing DNA base damage by downregulating DNA repair pathways.

140. Lamberti, G., et al., (2020) Targeting DNA damage response and repair genes to enhance anticancer immunotherapy: rationale and clinical implication. 16(23): p. 1751-1766.

141. Mandal, P.K., C. Blanpain, and D.J.J.N.R.M.C.B. Rossi, (2011) DNA damage response in adult stem cells: pathways and consequences. 12(3): p. 198-202.

142. Iliakis, G., et al., (2003) DNA damage checkpoint control in cells exposed to ionizing radiation. Oncogene. 22(37): p. 5834-5847.

143. Cramer, K., et al., (2008) BCR/ABL and other kinases from chronic myeloproliferative disorders stimulate single-strand annealing, an unfaithful DNA double-strand break repair. 68(17): p. 6884-6888.

144. Zhang, M., et al., (2008) Effects of fluoride on DNA damage, S-phase cell-cycle arrest and the expression of NF-κB in primary cultured rat hippocampal neurons. 179(1): p. 1-5.

145. Riffle, S., et al., (2017) Linking hypoxia, DNA damage and proliferation in multicellular tumor spheroids. 17(1): p. 1-12.

146. Dufau, I., et al., (2012) Multicellular tumor spheroid model to evaluate spatio-temporal dynamics effect of chemotherapeutics: application to the gemcitabine/CHK1 inhibitor combination in pancreatic cancer. 12(1): p. 1-11.

147. Mathews, L.A., et al., (2011) Increased expression of DNA repair genes in invasive human pancreatic cancer cells. 40(5): p. 730.

148. Masutani, C., et al., (1994) Purification and cloning of a nucleotide excision repair complex involving the xeroderma pigmentosum group C protein and a human homologue of yeast RAD23. 13(8): p. 1831-1843.

149. Sugasawa, K., et al., (2009) Two-step recognition of DNA damage for mammalian nucleotide excision repair: Directional binding of the XPC complex and DNA strand scanning. 36(4): p. 642-653.

150. Schärer, O.D.J.C.S.H.p.i.b., (2013) Nucleotide excision repair in eukaryotes. 5(10): p. a012609.

151. Bensimon, A., R. Aebersold, and Y. Shiloh, (2011) Beyond ATM: the protein kinase landscape of the DNA damage response. FEBS letters. 585(11): p. 1625-1639.

152. Pines, A., et al., (2012) PARP1 promotes nucleotide excision repair through DDB2 stabilization and recruitment of ALC1. 199(2): p. 235-249.

153. Jackson, S.P. and D. Durocher, (2013) Regulation of DNA damage responses by ubiquitin and SUMO. Molecular cell. 49(5): p. 795-807.

154. Povlsen, L.K., et al., (2012) Systems-wide analysis of ubiquitylation dynamics reveals a key role for PAF15 ubiquitylation in DNA-damage bypass. 14(10): p. 1089-1098.

155. Semenza, G.L.J.T.E.j., (2017) Hypoxia-inducible factors: coupling glucose metabolism and redox regulation with induction of the breast cancer stem cell phenotype. 36(3): p. 252-259.

156. Morimoto, H., et al., (2013) ROS are required for mouse spermatogonial stem cell self-renewal. 12(6): p. 774-786.

157. Owusu-Ansah, E. and U.J.N. Banerjee, (2009) Reactive oxygen species prime Drosophila haematopoietic progenitors for differentiation. 461(7263): p. 537-541.

158. Roesch, A., et al., (2010) A temporarily distinct subpopulation of slow-cycling melanoma cells is required for continuous tumor growth. 141(4): p. 583-594.

159. Ludwig, T., et al., (1997) Targeted mutations of breast cancer susceptibility gene homologs in mice: lethal phenotypes of Brca1, Brca2, Brca1/Brca2, Brca1/p53, and Brca2/p53 nullizygous embryos. 11(10): p. 1226-1241.

160. Sharan, S.K., et al., (1997) Embryonic lethality and radiation hypersensitivity mediated by Rad51 in mice lacking Brca2. 386(6627): p. 804-810.

161. Suzuki, A., et al., (1997) Brca2 is required for embryonic cellular proliferation in the mouse. 11(10): p. 1242-1252.

162. Cortez, D., et al., (1999) Requirement of ATM-dependent phosphorylation of brca1 in the DNA damage response to double-strand breaks. Science. 286(5442): p. 1162-1166.

163. Hohenstein, P., et al., (2001) A targeted mouse Brca1 mutation removing the last BRCT repeat results in apoptosis and embryonic lethality at the headfold stage. Oncogene. 20(20): p. 2544-2550.

164. Frankish, H., (2001) BRCA1 has a pivotal role in repairing DNA. The Lancet. 357(9269): p. 1678.

165. Snouwaert, J.N., et al., (1999) BRCA1 deficient embryonic stem cells display a decreased homologous recombination frequency and an increased frequency of non-homologous recombination that is corrected by expression of a brca1 transgene. 18(55): p. 7900-7907.

166. Connor, F., et al., (1997) Tumorigenesis and a DNA repair defect in mice with a truncating Brca2 mutation. Nature genetics. 17(4): p. 423-430.

167. Foray, N., et al., (1999) Gamma-rays-induced death of human cells carrying mutations of BRCA1 or BRCA2. Oncogene. 18(51): p. 7334-7342.

168. Wu, J., et al., (2010) The role of BRCA1 in DNA damage response. 1(2): p. 117-123.

Chapter Two: Evaluation of NADPH OXIDASE Inhibitors

Introduction

Reactive oxygen species and oxidative stress

Roughly 2.45 billion years ago, due to the oxygenic photosynthesis by cyanobacteria, the concentration of molecular oxygen in the earth's atmosphere started to increase. This led to the evolution of aerobic respiration and the development of complex eukaryotic organisms[1]. Over the past decades, it had been stated in various reports that oxygen-containing free radicals were responsible for toxic effects in aerobic organisms, referred to as oxidative stress or oxygen toxicity[2]. Reactive oxygen species (ROS) are a class of highly reactive molecules or free radicals generated through different cellular processes such as oxygen metabolism, respiration and under stress conditions. Among all the ROS, superoxide anion ($\bullet O_2-$), hydrogen peroxide (H_2O_2), and hydroxyl radicals ($\bullet OH$) are the most known examples. In contrast, other less popular examples are hypochlorous (HOCl), hypobromous (HOBr), and hypoiodous acids (HOI). Incorporation of peroxyl ($ROO\bullet$), alkoxy ($RO\bullet$), semiquinone ($SQ\bullet-$) and carbonate ($CO_3\bullet-$) radicals and organic hydroperoxides (ROOH) is also frequently encountered within the definition of ROS[3]. Different studies have demonstrated that

ROS is a messenger in cell signaling, including apoptosis, gene expression, and the activation of cell signaling cascades[4]. It has been implicated that ROS has been associated with various diseases triggered by oxidative stress, which occurs due to disruption of the balance between excessive formation of ROS and limited antioxidant defenses that directly damage numerous macromolecules such as nucleic acids, proteins, and non-saturated lipids in the cell. Under normal physiological conditions, the production of ROS is highly restricted to specific subcellular sites and is downregulated by several harmful feedback mechanisms. Production of ROS "in the wrong place at the wrong time" or generation of ROS in excessive amounts results in oxidative stress leading to cellular dysfunction and apoptosis, which contribute to atherosclerosis, heart failure, hypertension, ischemia/reperfusion injury, cancer, aging, and neurodegeneration. Although numerous enzyme systems produce ROS in mammalian cells, four enzymatic methods seem to predominate[5-7]. These include the NADPH oxidases, xanthine oxidase, uncoupled NO synthase, and the mitochondrial electron transport chain. There is a powerful interplay between these sources, such that activation of one can lead to activation of the others. The phenomenon of ROS-induced ROS production is very well documented: H_2O_2 activates $O_2\bullet-$ production by phagocytic and nonphagocytic NADPH oxidase; peroxynitrite uncouples endothelial NO synthase (eNOS), switching from NO to $O_2\bullet-$ production, and increases the production of mitochondrial ROS; and H_2O_2 induces transformation of xanthine dehydrogenase into xanthine oxidase, a source of H_2O_2 and $O_2\bullet-$[8]. The interplay between specific ROS sources, however, is not still evident.

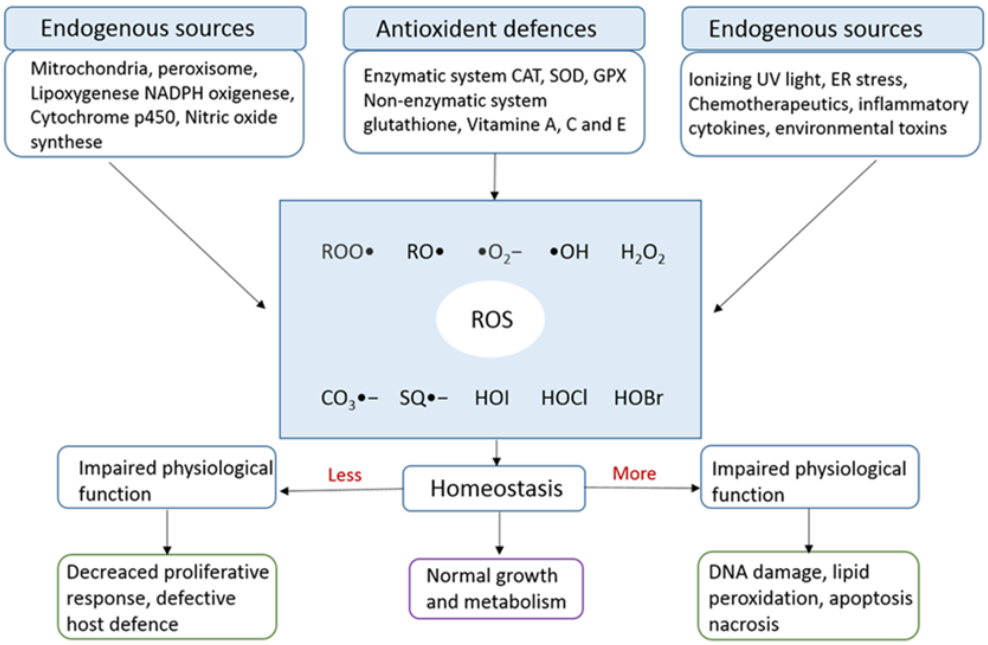

Figure 1. Sources of reactive oxygen species, antioxidant defence and subsequent biological effects depending on the level of ROS production.

NADPH Oxidases

NADPH oxidases are a family of enzyme complexes whose primary function is to catalyze the transfer of electrons from NADPH to molecular oxygen via their Nox catalytic subunit, generating O_2•− and H_2O_2 and represent the central control point for the regulation of the redox state. Over the past several years, it has become clear that reactive oxygen species (ROS) play an essential role in physiological and pathological processes. Nicotinamide adenine dinucleotide phosphate (NADPH Oxidase) is a

superfamily of enzymes consisting of 5 members NOX1, NOX2, NOX3 NOX4, NOX5, DUOX1, and DUOX2. They have been known to be critical producers of ROS. Out of the seven members of the NOX family, NOX1, NOX2, NOX3, and NOX5 are transmembrane proteins that function to transport electrons across biological membranes to reduce oxygen superoxide. At the same time, NOX4, DUOX1, and DUOX2 are producers of hydrogen peroxide (H_2O_2)[9,10]. Cellular reactive oxygen species (ROS) such as hydrogen peroxide (H_2O_2) and superoxide anion ($O_2 \bullet -$) are generally produced in response to cytokine or growth factor stimuli or as a by-product of mitochondrial oxidative phosphorylation.

The NOX enzymes contribute to numerous biological and pathological processes, including hearing and balance (NOX3), blood pressure regulation, inflammation, cell growth (NOX1/NOX2), and differentiation (NOX4). The NOX proteins vary in terms of their mode of activation and localization. NOX1 is expressed in smooth muscle cells but is also present in other vascular cells. NOX2, previously known as gp91phox, is present in endothelial and phagocytic cells. NOX3 is expressed in the brain and inner ear, while NOX4 is expressed and active in vascular smooth muscle and endothelial cells. NOX5 has been identified in immature human lymphatic tissues and endothelial cells, activated by Ca2+ binding to EF-hand motifs. The DUOX1/DUOX2 proteins possess a dual nature due to an extracellular peroxidase domain in addition to the EF-hand Ca_2+ binding and gp91phox homology domains[11].

Originally isolated from the thyroid, they produce the H_2O_2 used to oxidize iodide during thyroid hormone synthesis. NOXs are membrane proteins that share the same

catalytic core: a six transmembrane helical domain (TM) and a C-terminal cytosolic dehydrogenase domain (DH). DH contains the binding sites for FAD (flavin adenine dinucleotide) and NADPH, whereas TM binds two hemes. The enzyme catalytic cycle entails a series of steps, which sequentially transfer electrons from cytosolic NADPH to an oxygen-reducing centre located on the extra cytoplasmic side of the membrane[12]. Thus, a distinctive feature of NOXs is that NADPH oxidation and ROS production take place on the opposite sides of the membrane. Structurally, NADPH oxidase is a multicomponent enzyme that includes two integral membrane proteins, glycoprotein gp91 Phox and adaptor protein p22(phox), which form the heterodimeric flavocytochrome b558 that constitutes the core of the enzyme. During the resting state, the multidomain regulatory subunits p40(phox), p47(phox), p67(Phox) are in the cytosol organized as a complex.

The activation of phagocytic NADPH oxidase occurs through a complex series of protein interactions. The role of NOX has also been well established under non-pathological conditions. Vascular NOX generates ROS essential for maintaining normal cardiovascular health through regulating blood pressure, which is vital to health, as aberrations from normal levels can be lethal. The presence of ROS reduces the bioavailability of the endothelial-derived relaxation factor, nitric oxide (NO), which regulates blood pressure. In normal kidneys, ROS is produced through NOX3, and these molecules regulate renal function through the control of Na+ transport, tubuloglomerular feedback, and renal oxygenation. Furthermore, oxygen radicals increase $NaCl_2$ absorption in the loop of Henle, resulting in the modulation of Na+/H+

exchange. Pulmonary NOX2 has been implicated in the airway and vascular remodeling. The p22phox-dependent NOX2 regulates the proliferation and differentiation of smooth muscle cells through the activation of nuclear factor kappa B (NF-κB) and inducible nitric oxide synthase (iNOS). ROS generation through DUOX and NOX1 in the colon mucosa promotes serotonin biosynthesis, essential in regulating secretion and motility. NOX2 is involved in the normal functioning of the central nervous system through angiotensin II signaling in the nucleus tractus solitarius and the hypothalamic cardiovascular regulator nuclei. Moreover, microglial cells express NOX2 and p22phox, and both enzymes regulate microglial proliferation and neuronal apoptosis during nerve growth factor deprivation.

NOX Regulation of Cancer Stem Cells

One of the major sources of reactive oxygen species (ROS) generated within stem cells is the nicotinamide adenine dinucleotide phosphate (NADPH) oxidase family of enzymes (NOXs), which are critical determinants of the redox state beside antioxidant defense mechanisms [13]. This balance is involved in another one that regulates stem cell fate: indeed, self-renewal, proliferation, and differentiation are decisive steps for stem cells during embryo development, adult tissue renovation, and cell therapy application. Ex vivo culture-expanded stem cells are being investigated for tissue repair and immune modulation, but events such as aging, senescence, and oxidative stress reduce their ex vivo proliferation, which is crucial for their clinical applications. Many types of cultured cancer cell lines and human tumors at early and late stages of tumorigenesis express higher levels of NOX1, NOX2, NOX4, and NOX5 or their regulatory components

compared with normal controls, suggesting a pivotal role either in cancer development or in progression[14]. Cancer stem cells (CSCs) are involved in various tumorigenic process such as invasion, metastasis, angiogenesis, and resistance to chemotherapy. In contrast to cancer cells, which have elevated ROS levels, CSCs generally maintain low levels of intracellular ROS by means of various mechanism[13,15].

Unfortunately, tumor-initiating cells (TICs)/or cancer stem cells seem to be the most malignant cell subpopulation in tumors because of their resistance to chemotherapy or radiation treatment. Therefore, a potential key innovation for cancer treatment is represented by targeting TICs[16,17]. In particular, Liu and Colleague showed that PPARγ agonists inhibited the cancer stem cell-like phenotype and decreased tumor growth of human hepatocellular carcinoma (HCC) cells. The increase in NOX2-derived ROS was partially responsible for the inhibitory effects mediated by PPARγ agonists. Nevertheless, ROS generation induced by PPARγ agonist significantly activated Akt, which in turn led to TIC survival by limiting ROS generation. Therefore, much remains to be learned about this topic, and not only NOX2 but also the role played by other isoforms should be considered; this represents a limit of this study, that otherwise suggests a potential treatment of liver cancer based on a combinatory strategy involving an Akt inhibitor and a PPARγ agonist for inhibition of stem cell-like properties in HCCs. Focusing now on a different and non-solid tumor, it is difficult to identify a single driving force for leukemogenesis since it is a multistep process[18]. However, the increased production of intracellular ROS characteristics of tumor cells is also a feature of leukemic cells. Elevated intracellular ROS level is indeed a feature observed in

numerous leukemic cell lines and in the cells from patients with different types of leukemia[19]. As previously reported, a low level of ROS is important for maintaining quiescence and the differentiation potential of hematopoietic stem cells (HSCs), whereas the level of ROS increases during hematopoietic differentiation. Analogously, in acute myeloid leukemia (AML), a low level of ROS is associated with leukemic stem cell (LSC) quiescence, whereas a high level promotes blast proliferation[20]. An interesting study, suggesting that cancer stem cells are known to mediate metastasis and recurrence and are therefore a promising therapeutic target, is focused on the CSC inhibitory effect of dihydrotanshinone (DHTS) that involves NOX5 activation. NOX5-derived ROS induced by DHTS deregulated the Stat3/IL-6 pathway, leading to CSC death. Since cell transformation frequently relies on NADPH oxidase-driven ROS production, NADPH oxidases appear to be suitable therapeutic targets in leukemia as recently reported. In this context, preclinical data show that the inhibition of NADPH oxidases is an effective strategy to block the signaling cascades initiated by the BCR-ABL and FLT3-ITD oncokinases in CML and AML cells, respectively. Thus, the use of TKis and NADPH oxidase inhibitors presents a strong synergistic effect. As discussed above, several oncogenes increase ROS production through NADPH oxidases, which turns these enzymes into desirable targets against leukemia[21-23]. Taken together, results suggest distinct and specific signals and effects for NOX family enzymes not only in leukemia but also in various oncogenic mechanisms, which deserve to be elucidated, to find out effective therapies.

Enrichment of a population of breast cancer stem-like cell population, induced by exposure to low concentrations of combined carcinogens, correlates with the activation of the RAS-Erk1/2-NOX1 pathway which plays an important role in maintaining increased cell proliferation[24]. The opposite result was observed for stem-like holoclones derived from the PC3 human prostate cancer cell line, which showed reduced expression of NOX2, NOX4, and NOX5, and their upregulation significantly lowered cell survival in vitro. Gemcitabine, a chemotherapeutic drug used in advanced pancreatic cancer, is characterized by low efficiency, and causes rapid development of chemoresistance. New data show that the pancreatic cancer stem cell phenotype (characterized by CD44+, CD24+, and CD133+ markers) can be induced by gemcitabine itself. Gemcitabine activates the NF-κB/STAT3 signaling cascade through NOX-mediated production of ROS, and pancreatic cell lines incubated with the NOX inhibitor apocynin show not only a decrease in ROS and p-STAT3 levels but also an abolished expression of Nanog, Sox2, and Bmi1, genes associated with self-renewal and maintaining pluripotency. NOX2 has been suggested as a potential target in the development of a therapy against chronic myeloid leukemia (CML) and glioblastoma, as the resistance of CML stem cells and patient-derived glioblastoma stem cells to tyrosine kinase inhibitors seem to be mediated through the NOX2/Egr1/Fyn axis[25]. Chemotherapy may induce the overproduction of ROS which leads to NF-κB-mediated release of inflammatory cytokines, including IL-6 and IL-8, and drive cancer progression through inflammation. Additionally, interleukin-6 is known to induce resistance of myeloma cells to chemo- and radiotherapy by NF-κB-dependent increase of

manganese superoxide dismutase expression (MnSOD). Unfortunately, there is not enough data to confirm whether such re-establishing of redox homeostasis exist in cancer stem cells[26]. The role of NOX-generated ROS in the functioning of cancer stem cells is not well understood yet, but considering their role in cancer recurrence and chemo- and radiotherapy resistance, this seems to be one of the most important research areas in current oxidative medicine.

In this study

In this study the NOX inhibitors Apocynin, G4 and G6, VAS2870, Diphenyaliodonium chloride (DPI), ATPsynthase inhibitor Oligomycin, iron chelators Deferoxamine and Deferasirox to evaluate anti CSC effect. NOX inhibitors G4 and G6 are patented and designed by Glucox Biotech AB. The substance G4 inhibits both Nox2 and Nox4 enzymes, whereas the inhibitors G6 inhibits NOX2 only. Apocynin and VAS2870 is known to knock down all the NADPH oxidase enzymes. In this experimental design effect, the of these 8 drugs were evaluated in the miPS-HuhcmP cancer stem cell models. The cancer stem cell models were derived from miPS cells without any without any genetic manipulation [27].

Aim of the Study

The aim of the experimental design is to evaluate the effect of the NOX inhibitors Apocynin, Diphenyleneiodonium chloride (DPI), GLX7013144 (G4), GLX7012166(G6) and, VAS2870, Oligomycine, Deferoxamine and Deferasirox using 2D culture condition. The hypothesis is that, reducing the enzymatic activity of Nox will decrease the viability

of the miPS-LLCcmP and miPS-Huh7cmP cells by down regulating the production and levels of ROS. The purpose of the study is to evaluate the efficacy of the new substances provided by the Glucose Biotech AB for treatment of cancer, by targeting the NADPH oxidase enzymatic activity in Cancer.

2. Materials and Methods

2.1 Cell culture

The miPS-Huh7cmP cells was obtained by the conversion of miPSCs (iPS-MEF-Ng-20D-17, Lot No. 012, Riken Cell Bank, Tokyo, Japan) with the conditioned media of human liver cancer cell line Huh7 cells [14]. Since GFP gene is originally integrated into the genome together with nanog promoter puromycin (puro) resistant gene, GFP expression was controlled by the stages of differentiation of the cells. Also, in the presence of puro, the cells were considered undifferentiated with GFP expression. miPS-Huh7cmP cells were maintained on 1% gelatin-coated 60 mm-dishes in miPS medium consisting of DMEM (Wako, Tokyo, Japan), 15% fetal bovine serum (FBS) (Thermo-Fischer, CA), 0.1 mM MEM non-essential amino acids (NEAA) (Gibco, Waltham, MA, USA), 2 mM L-glutamine (Nacalai Tesque, Kyoto, Japan) and 0.1 mM 2-mercaptoethanol (Merck-Millipore, MA, USA) supplemented with 50 U/mL penicillin/streptomycin 14 (Wako-Fujifilm, Japan). In this study cells were cultured in an incubator at 37°C in 5% CO_2 atmosphere.

2.2 Chemical compound

Diphenyleiodonium chloride (DPI) (CAS No. 4673-26-1, Tocris bioscience, UK) was dissolved in dimethyl sulfoxide (DMSO) (Wako, Japan) and stored at −20°C until use. VAS2870 (Funakoshi Co., Ltd. CAS: 722456-31-7, Tokyo) was dissolved in dimethyl sulfoxide (DMSO) and stored at −20° C until use. GLX7013144 and GLX7012166 were obtained from Glucox Biotech AB.

2.3 Cell proliferation assay

To measure the cell proliferation, 500 miPS-Huh7cmP cells were seeded per well in 96-well plates (TPP, Switzerland) and incubated overnight at 37 °C. After 24 hr the media was changed to medium containing varying concentrations of DPI and the incubation was further continued. After 12hr of incubation with drug, 5mg/mL of 3-[4,5-dimethylthiazol-2yl]-2,5-diphenyl-tetrazolium bromide (MTT) (Dojin, Japan) in PBS was added at a final concentration of 0.5 mg/mL in each well and the plate and incubated for 4 hr. Formed formazan crystals were dissolved with 10% w/v SDS in 0.02 N HCl by incubating overnight. Then the absorbance of each well was measured at 570 nm using MTP-800 Lab microplate reader (Corona Electric, Ibaraki, Japan). All the experiments were performed in triplicate. Cell viability was calculated relative to the untreated cells. IC50 values were estimated from the survival curve.

2.4 Statistical analysis

Normal distribution (Shapiro–Wilk test) and homogeneity of variances (Brown Forsythe test) were performed. One way ANOVA was used to analyze the results. All statistical analyses were performed with Prism 7 (Graph Pad Software, CA), at a significance level of 5% ($P < 0.05$). Data were represented as mean ± SD.

Results

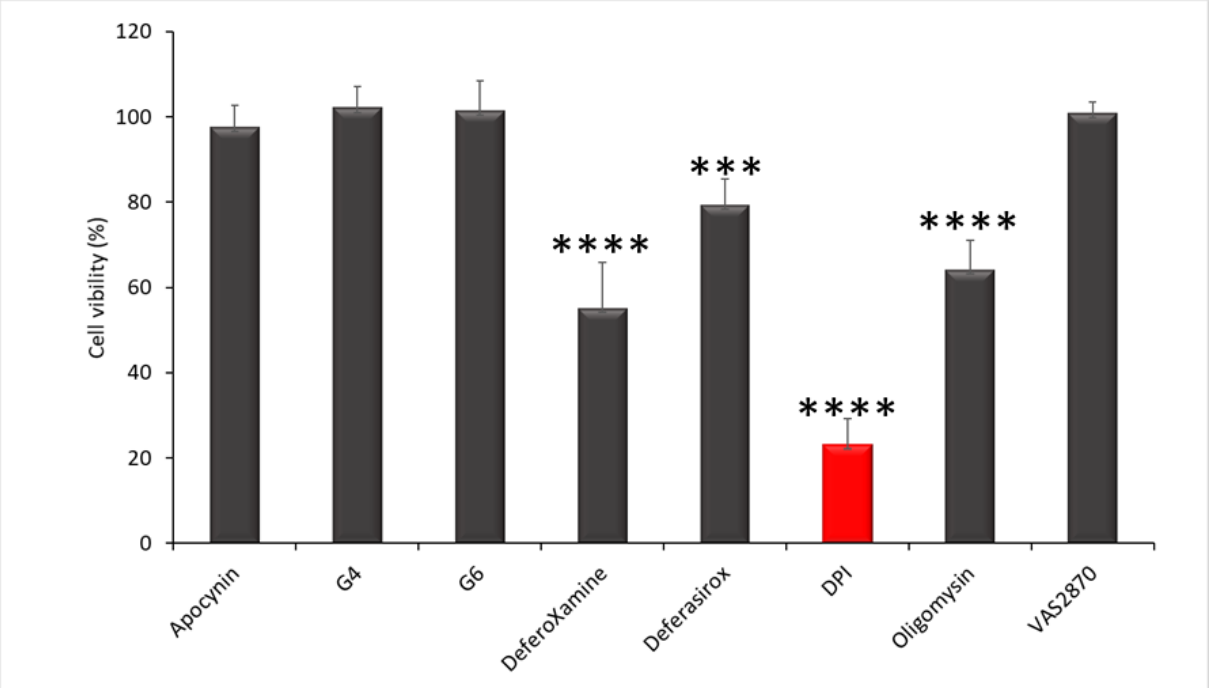

Figure 2: Bar Graph representing cell viability of miPS-HuhcmP cells in 1µM concentration of Apocynin, G4, G6, Deferoxamine, Deferasirox, DPI, Oligomycin, VAS2870.

The drug concentration at 1µM and the miPS-Huh7cmP cells were treated with all the inhibitors with for 12 hours. Apocynin (97.57 ± 5.1, p=0.403), G4 (102 ± 10.70. p= 0.4.43), G6 (101.31 ± 6.11, p= 0.211) and VAS2870 (100.825 ± 0.455) showed no effect on the miPIS-HUH7cmP cells, whereas Deferoxamine (55.06 ± 5.99, p= 0.0001), Deferasirox (79.23 ± 6.88, p= 0.064), DPI (23.15 ± 0.002) and Oligomycin (64.166 ± 8.7 p= 0.01) had significantly reduced the viability of the cells, Out of the 8 drugs tested DPI has the lowest viability rate (Figure 2).

Discussion

We were screening for NADPH oxidases that were that would show significant amount reduction in cell proliferation in thew concentration of 1µM. Apocynin is a naturally occurring acetophenone, found in the roots of *Apocynum cannabinum* and *Picrorhiza kurroa*. Apocynin has been primarily reported as an NADPH oxidase (NOX) inhibitor and prevents translocation of its p47phox subunit to the plasma membrane, observed in neurodegeneration and hypertension. However, recent studies highlight its off-target effects that it can function as a scavenger of non-radical oxidant species, which is relevant for its activity against NOX 4 mediated production of hydrogen peroxide [28,29]. Apocynin showed no anti-CSC effect on the CSC model miPS-Huh7cmP cells. VAS2870 has been previously reported to show anti-cancer effect. However in the cancer stem

cell model miPS-Huh7cmP cells in 1µM concentration did not show any effect on reduction of cell proliferation [30,31]. Cancer cells have upregulated glycolysis compared with normal cells, which has led many to the assumption that oxidative phosphorylation (OXPHOS) is downregulated in all cancers. Oligomycin is knows as an ATP-synthase blocker which targets OXPHOS. Our results indicate that Oligomycin inhibits CSC proliferation by 40% in that 1µM concentration [32-34] .Deferoxamine is an organic compound derived from the bacterium *Streptomyces pilosus* and can chelate iron and had been previously reported to how anti-cancer stem cell effect [35,36]. Dereroxamine reduced the cell viability by 55% and Deferasirox reduced the cell viability by 20%. NADPH oxidases have a heme binding domain. We hypnotized that the iron chelators would partially inhibit anti-CSC effect. Diphenyeliodonium chloride is a renounced NADPH oxidase inhibitor and also a potent mitochondrial complex 2 inhibitor [37,38] . In the liver cancer stem cell model miPSHuh7cmP cells DPI decreased proliferation of the cells by 80% while only 20% of the cells had been alive in the frame of 12hr treatment.

Conclusion

Based on the drugs evaluated we chose DPI as out target candidate for checking the anti-CSC effect.

Reference

1. Falkowski PGJS. Tracing oxygen's imprint on Earth's metabolic evolution. 2006;311(5768):1724-1725.
2. Gerschman R, Gilbert DL, Nye SW, Dwyer P, Fenn WOJS. Oxygen poisoning and x-irradiation: a mechanism in common. 1954;119(3097):623-626.
3. Krumova K, Cosa G. Overview of reactive oxygen species. 2016.
4. Jakubczyk K, Dec K, Kałduńska J, Kawczuga D, Kochman J, Janda KJPmloPTL. Reactive oxygen species-sources, functions, oxidative damage. 2020;48(284):124-127.
5. De Deken X, Corvilain B, Dumont JE, Miot FJA, signaling r. Roles of DUOX-mediated hydrogen peroxide in metabolism, host defense, and signaling. 2014;20(17):2776-2793.
6. Smeyne M, Smeyne RJJFRB, Medicine. Glutathione metabolism and Parkinson's disease. 2013;62:13-25.

7. Aliev G, Priyadarshini M, P Reddy V, et al. Oxidative stress mediated mitochondrial and vascular lesions as markers in the pathogenesis of Alzheimer disease. 2014;21(19):2208-2217.
8. Auten RL, Davis JMJPr. Oxygen toxicity and reactive oxygen species: the devil is in the details. 2009;66(2):121-127.
9. Bedard K, Krause K-HJPr. The NOX family of ROS-generating NADPH oxidases: physiology and pathophysiology. 2007;87(1):245-313.
10. Konior A, Schramm A, Czesnikiewicz-Guzik M, Guzik TJJA, signaling r. NADPH oxidases in vascular pathology. 2014;20(17):2794-2814.
11. Magnani F, Nenci S, Fananas EM, et al. Crystal structures and atomic model of NADPH oxidase. 2017;114(26):6764-6769.
12. Taylor WR, Jones DT, Segal AWJPS. A structural model for the nucleotide binding domains of the flavocytochrome b–245 β-chain. 1993;2(10):1675-1685.
13. Juhasz A, Ge Y, Markel S, et al. Expression of NADPH oxidase homologues and accessory genes in human cancer cell lines, tumours and adjacent normal tissues. 2009;43(6):523-532.
14. Galadari S, Rahman A, Pallichankandy S, Thayyullathil FJFRB, Medicine. Reactive oxygen species and cancer paradox: to promote or to suppress? 2017;104:144-164.
15. Zhang Z, Duan Q, Zhao H, et al. Gemcitabine treatment promotes pancreatic cancer stemness through the Nox/ROS/NF-κB/STAT3 signaling cascade. 2016;382(1):53-63.
16. Li F, Tiede B, Massagué J, Kang YJCr. Beyond tumorigenesis: cancer stem cells in metastasis. 2007;17(1):3-14.
17. Kreso A, Dick JEJCsc. Evolution of the cancer stem cell model. 2014;14(3):275-291.
18. Liu L, Yang Z, Xu Y, et al. Inhibition of oxidative stress-elicited AKT activation facilitates PPARγ agonist-mediated inhibition of stem cell character and tumor growth of liver cancer cells. 2013;8(8):e73038.

19. Zhou Y, Hileman EO, Plunkett W, Keating MJ, Huang PJB, The Journal of the American Society of Hematology. Free radical stress in chronic lymphocytic leukemia cells and its role in cellular sensitivity to ROS-generating anticancer agents. 2003;101(10):4098-4104.
20. Al-Gayyar MM, Eissa LA, Rabie AM, El-Gayar AMJJop, pharmacology. Measurements of oxidative stress status and antioxidant activity in chronic leukaemia patients. 2007;59(3):409-417.
21. Hole PS, Zabkiewicz J, Munje C, et al. Overproduction of NOX-derived ROS in AML promotes proliferation and is associated with defective oxidative stress signaling. 2013;122(19):3322-3330.
22. Prata C, Facchini C, Leoncini E, et al. Sulforaphane modulates AQP8-linked redox signalling in leukemia cells. 2018;2018.
23. Dakik H, El Dor M, Leclerc J, et al. Characterization of NADPH Oxidase Expression and Activity in Acute Myeloid Leukemia Cell Lines: A Correlation with the Differentiation Status. 2021;10(3):498.
24. Kim S-L, Choi HS, Kim J-H, et al. Dihydrotanshinone-induced NOX5 activation inhibits breast cancer stem cell through the ROS/Stat3 signaling pathway. 2019;2019.
25. Prieto-Bermejo R, Romo-González M, Pérez-Fernández A, Ijurko C, Hernández-Hernández ÁJJoE, Research CC. Reactive oxygen species in haematopoiesis: leukaemic cells take a walk on the wild side. 2018;37(1):1-18.
26. Sánchez-Sánchez B, Gutiérrez-Herrero S, López-Ruano G, et al. NADPH oxidases as therapeutic targets in chronic myelogenous leukemia. 2014;20(15):4014-4025.
27. Afify SM, Chen L, Yan T, et al. Method to convert stem cells into cancer stem cells. 2019;2(3):71.
28. Stefanska J, Pawliczak RJMoi. Apocynin: molecular aptitudes. 2008;2008.
29. Paul S, Chakrabarty S, Ghosh S, et al. Targeting cellular microtubule by phytochemical apocynin exhibits autophagy-mediated apoptosis to inhibit lung carcinoma progression and tumorigenesis. 2020;67:153152.

30. Sancho P, Fabregat IJBp. The NADPH oxidase inhibitor VAS2870 impairs cell growth and enhances TGF-β-induced apoptosis of liver tumor cells. 2011;81(7):917-924.
31. Weyemi U, E Redon C, R Parekh P, Dupuy C, M Bonner WJA-CAiMC. NADPH Oxidases NOXs and DUOXs as putative targets for cancer therapy. 2013;13(3):502-514.
32. Symersky J, Osowski D, Walters DE, Mueller DMJPotNAoS. Oligomycin frames a common drug-binding site in the ATP synthase. 2012;109(35):13961-13965.
33. Bonuccelli G, Peiris-Pages M, Ozsvari B, Martinez-Outschoorn UE, Sotgia F, Lisanti MPJO. Targeting cancer stem cell propagation with palbociclib, a CDK4/6 inhibitor: Telomerase drives tumor cell heterogeneity. 2017;8(6):9868.
34. Gao C, Shen Y, Jin F, Miao Y, Qiu XJPO. Cancer stem cells in small cell lung cancer cell line H446: higher dependency on oxidative phosphorylation and mitochondrial substrate-level phosphorylation than non-stem cancer cells. 2016;11(5):e0154576.
35. Szymonik J, Wala K, Górnicki T, Saczko J, Pencakowski B, Kulbacka JJIJoMS. The Impact of Iron Chelators on the Biology of Cancer Stem Cells. 2022;23(1):89.
36. Ninomiya T, Ohara T, Noma K, et al. Iron depletion is a novel therapeutic strategy to target cancer stem cells. 2017;8(58):98405.
37. Zavadskis S, Weidinger A, Hanetseder D, et al. Effect of Diphenyleneiodonium Chloride on Intracellular Reactive Oxygen Species Metabolism with Emphasis on NADPH Oxidase and Mitochondria in Two Therapeutically Relevant Human Cell Types. 2021;13(1):10.
38. Ozsvari B, Bonuccelli G, Sanchez-Alvarez R, Foster R, Sotgia F, Lisanti MPJA. Targeting flavin-containing enzymes eliminates cancer stem cells (CSCs), by inhibiting mitochondrial respiration: Vitamin B2 (Riboflavin) in cancer therapy. 2017;9(12):2610.

Chapter Three: Diphenyleneiodonium efficiently inhibits the characteristics of a cancer stem cell model derived from induced pluripotent stem cells

Abstract

Diphenyleneiodonium (DPI) has long been evaluated as an anti-cancer drug inhibiting NADPH oxidase, the IC_{50} in several cancer cell lines were reported 10 μM, which is too high for efficacy. In this study, we employed miPS-Huh7cmP cells, which we previously established as a cancer stem cell (CSC) model from induced pluripotent stem cells, to reevaluate the efficacy of DPI because CSCs are currently one of the main foci of therapeutic strategy to treat cancer, but generally considered resistant to chemotherapy. As the results, the conventional assay for the cell growth inhibition by

DPI accounted for an IC_{50} at 712nM that was not enough to define the effectiveness as an anti-cancer drug. Simultaneously, wound healing assay revealed an IC_{50} of approximately 500 nM. Comparatively, the IC_{50} values shown on sphere formation, colony formation, and tube formation assays were 5.52, 12 and 8.7 nM, respectively. However, these inhibitory effects were not observed by VAS2780, also a reputed NADPH oxidase inhibitor. It is noteworthy that these three assays are evaluating the characteristic of CSCs and are designed in the 3D culture methods. We concluded that DPI could be a suitable candidate to target mitochondrial respiration in CSCs. We propose that the 3D culture assays are more efficient to screen anti-CSC drug candidates and better mimic tumor microenvironment when compared to the adherent monolayer of 2D culture system used for a conventional assay, such as cell growth inhibition and wound healing assays.

Significance of study

Diphenyleneiodonium (DPI) is NADPH oxidase inhibitor. Here we revaluate DPI as an anticancer drug by assessing its effect on iPS derived cancer stem cell model in both 2D and 3D culture conditions. Our data showed that DPI inhibited the four major characteristics, self-renewal, differentiation, tumorigenic and migration potential of the cancer stem cell model, strengthening its position as a potent anticancer drug**.**

1. Introduction

Cancer stem cells (CSCs), also known as tumor initiating cells, exhibit self-renewal properties, tumorigenicity, and multilineage differentiation capacity, have been found to be responsible for cancer relapse and metastasis. CSCs can evade treatments like chemo- and radiotherapy which make the morbidity and mortality rate poor. Although CSCs are important targets for therapy, clinically effective targeting strategies have not yet been established due to the therapeutic resistance. This is because of the low number of CSCs in each tumor tissue which is one of the substantial problems to obtain enough amounts of cells to be studied well. Our group has been working on the establishment of novel CSC models from pluripotent stem cells [1]. These cells were epigenetically converted from pluripotent stem cells without genetic manipulations under the mimic of cancer inducing microenvironment. The method of CSC preparation has the advantage producing various types of CSCs not only with

mutations but also with epigenetic alterations based on the naturally occurring events such as chronic inflammation involving different growth factors, cytokines, chemokines etc. The CSCs derived from iPSCs can reflect the patient genetic background than those obtained from experimental genetic manipulation. And this method allowed us to establish CSC models under various conditions of microenvironments, so that it become possible to evaluate the efficacy of the drugs against CSCs in easier ways than before [2-4]. Currently, many aspects of the targets in a CSC are conceivable to design a drug against CSCs [5]. Sometimes the apoptosis inhibiting topoisomerase with Daunorubicin/Doxorubicin [4], sometimes the dynamics of tubulins inhibiting with Paclitaxel and others cytoplasmic signaling have been evaluated [6]. The metabolic pathways are also considered as good target candidates [7]. Typically, glycogenesis could be related with Warburg effects leading to ATP production in anaerobic conditions. However, ATP production is generally constitutive through both glycogenesis and mitochondrial TCA cycle coupled with electron transport system [8]. In this energy production process NADPH oxidation is essential to salvage NADH, so that inhibition of this process would be one of the targets to treat CSCs [9-11]. To answer the purpose, Diphenyleneiodonium chloride (DPI) was employed in this study as a candidate to inhibit NADPH oxidase resulting in the depletion of NADH attenuating ATP synthesis [12]. We tried to assess the effect of DPI on the CSC properties using miPS-Huh7cmP cells which were established as CSCs from mouse induced pluripotent stem cells (miPSCs) in the presence of the conditioned medium of human liver cancer cell line Huh7 cells [13].

VAS2870 was used as a reference molecule of NADPH oxidase inhibitor which specifically blocks the NOX isoforms but does not inhibit mitochondrial ATP synthesis.

2. Materials and Methods

2.1 Cell culture

The miPS-Huh7cmP cells was obtained by the conversion of miPSCs (iPS-MEF-Ng-20D-17, Lot No. 012, Riken Cell Bank, Tokyo, Japan) with the conditioned media of human liver cancer cell line Huh7 cells [14]. Since GFP gene is originally integrated into the genome together with nanog promoter puromycin (puro) resistant gene, GFP expression was controlled by the stages of differentiation of the cells. Also, in the presence of puro, the cells were considered undifferentiated with GFP expression. miPS-Huh7cmP cells were maintained on 1% gelatin-coated 60 mm-dishes in miPS medium consisting of DMEM (Wako, Tokyo, Japan), 15% fetal bovine serum (FBS) (Thermo-Fischer, CA), 0.1 mM MEM non-essential amino acids (NEAA) (Gibco, Waltham, MA, USA), 2 mM L-glutamine (Nacalai Tesque, Kyoto, Japan) and 0.1 mM 2-mercaptoethanol (Merck-Millipore, MA, USA) supplemented with 50 U/mL penicillin/streptomycin [14] (Wako-Fujifilm, Japan). In this study cells were cultured in an incubator at 37°C in 5% CO_2 atmosphere.

2.2 Chemical compound

Diphenyleiodonium chloride (DPI) (CAS No. 4673-26-1, Tocris bioscience, UK) was dissolved in dimethyl sulfoxide (DMSO) (Wako, Japan) and stored at −20°C until use.

VAS2870 (Funakoshi Co., Ltd. CAS: 722456-31-7, Tokyo) was dissolved in dimethyl sulfoxide (DMSO) and stored at −20° C until use.

2.3 Cell proliferation assay

To measure the cell proliferation, 500 miPS-Huh7cmP cells were seeded per well in 96-well plates (TPP, Switzerland) and incubated overnight at 37 °C. After 24 hr the media was changed to medium containing varying concentrations of DPI and the incubation was further continued. After 12hr of incubation with drug, 5mg/mL of 3-[4,5-dimethylthiazol-2yl]-2,5-diphenyl-tetrazolium bromide (MTT) (Dojin, Japan) in PBS was added at a final concentration of 0.5 mg/mL in each well and the plate and incubated for 4 hr. Formed formazan crystals were dissolved with 10% w/v SDS in 0.02 N HCl by incubating overnight. Then the absorbance of each well was measured at 570 nm using MTP-800 Lab microplate reader (Corona Electric, Ibaraki, Japan). All the experiments were performed in triplicate. Cell viability was calculated relative to the untreated cells. IC_{50} values were estimated from the survival curve.

2.4 Sphere formation

Self-renewal potential was evaluated by sphere-formation in non-adhesive conditions. Cells were seeded at 10000 cells/well and maintained on 24-well ultra-low attachment surface plates (Coaster 24-well plate, Corning, ME) in serum-free DMEM supplemented with insulin-transferrin-selenium-X (ITS-X) (1/100 v/v, Life Technologies, Carlsbad, CA, USA), 0.1 mM NEAA, 2 mM L-glutamine, 0.1 mM 2-mercaptoethanol and 50 U/mL penicillin/streptomycin supplemented with different concentration of DPI. After 5 days, from each well the number of the spheres with diameter ≥50 μm was counted

with Metamorph Imaging software (Molecular Devices, UK). Images were captured with an IX81 inverted microscope equipped with a fluorescence device (Olympus, Tokyo, Japan).

2.5 Clonogenic assay

To assess the colony formation, cells were seeded at 500 cells/dish on gelatin-coated 35-mm dishes (TPP, Switzerland). After 24 hr of incubation, different concentrations DPI was added to each dish and culture was continued up to 10 days until milky white colonies appeared. Then the colonies were fixed using 75% methanol (Nacaclai Tesque, Japan) and stained with 7.5 % w/v Giemsa (Sigma-Aldrich, MO) in glycerol/methanol (1+1).

2.6 *In vitro* tube formation assay

Coverslips coated with Matrigel (Corning Inc., NY) were prepared in a 24-well plate (TPP, Switzerland). The miPS-Huh7cmP cells were suspended in endothelial basal medium EBM2 (Lonza, Switzerland) supplemented with 2% FBS, seeded at $5x10^5$ cells/well in presence or absence of DPI and VAS2870, and incubated at 37°C in the atmosphere of 5% CO_2. After 24 hours, tube formation was observed under an IX81 inverted microscope equipped with fluorescence apparatus (Olympus, Japan). After washed with PBS, the cells were fixed with 4% paraformaldehyde for 20min at 25°C. Then the cells were blocked with 5% FBS for 20 min at 25°C and stained with anti-CD31 rabbit polyclonal antibody (ab28364, Abcam, UK) overnight at 4°C. Next, the cells were washed with PBS and incubated with goat anti-rabbit IgG antibody labelled with Alexa Fluor™ 555 (A-21428, Life 238 Technology, CA). After being washed with PBS,

coverslips were mounted on slides with mounting solution with DAPI and images were observed under an FSX100 inverted fluorescence microscope (Olympus, Japan).

2.7 Scratch wound-healing assay

Prior to the wound healing assay, the doubling time of the cells were estimated as following. miPS-Huh7cmP cells in mouse iPS media were seeded into 35-mm dishes at a density of 20,000 cells/dish coated with gelatine. The cells were incubated at 37°C in 5% CO_2 atmosphere. At very 24 hr up to 96 hr, the cells were trypsin zed and counted by Trypan Blue exclusion method with a haematocytometer under an optical microscope. The doubling time was estimated by the equation by Roth V., 2006, Doubling Time Computing <http://www.doubling-time.com/compute.php> to be 14.9± 2.5 hr. Then, cells were seeded in 60-mm dishes at 5×10^5 cells/dish and incubated for 24 hr to allow formation of a confluent monolayer. Then the confluent cell sheet was wounded by scratching off the bottom of culture with a 200-µL pipette tip. The peeled-off cells were washed three times with PBS to be detached and to remove any floating cell debris. Then the media was changed to 5% FBS DMEM supplemented with varying concentration of DPI or VAS2870 and the cell migration was monitored at 12 hr and images of wound healing were captured with a IX81 inverted microscope. Images were analyzed using ImageJ and the area of the wound healed was measured.

2.8 Flowcytometric analysis

The presence of GFP positive and negative cells in the population of cells was assessed by a BD AccuriTM C6 plus Flow Cytometer (Becton & Dickinson, MA). The trypsinized cells were washed, resuspended in PBS containing 10% FBS and applied to the flow

cytometer. To analyze the cell cycle, cells were harvested after treating with DPI for 48 hr, fixed in ice cold 70% ethanol and permeabilized followed by staining with propidium iodide (PI) (Sigma-Aldrich, NY) at either 37°C for 15 min [15]. Then the cells were passed through nylon mesh to remove aggregated cells and applied to the flow cytometer. The data were analyzed using the FlowJo® software (FlowJo, LLC, Ashland, OR).

2.9 Western Blot

To begin with $5x10^5$ cells were seeded on 6cm dishes and treated with DPI for 48 hr. Then cells were harvested and lysed using lysis buffer consisting of 50nM tris-HCL, pH 7.4, 15-nM NaCl, 5nM ETDA, 1% Triton X-100 (Wako, Japan) and 1 µg/ml phosphatase inhibitor (Nakalai Tesque, Japan). After that protein concentration was quantified using BCA protein assay kit (Thermo Fisher, CA). The protein samples were fractionated using 12.5% SDS-PAGE and then transferred on to PVDF membranes (Immobilon-FL, Merck Millipore, Germany) from the Gel. Followed by membrane transfer, the membranes were blocked in 5% non-fat skimmed milk (Snow Brand, Japan) in 20 mM Tris-HCl, pH 7.6, 150 mM NaCl, and 0.05% Teen 20 (TBST). After blocking the membranes, they were incubated with primary antibodies overnight at 4°C. After washing the excess primary antibody away with skimmed milk, the membranes were washed with horseradish peroxidase (HRP)-conjugated secondary antibodies for 1 hr at room temperature. Signals from the stained membranes were visualized using a chemiluminescent horseradish peroxidase (HRP) substrate EzWestLumi plus (ATTO, Japan) and finally images were taken using a WSE-6100 LuminoGraph (ATTO, Japan)

using different exposure. Endogenous β-actin was considered used as an internal control. The images were analysed with ImageJ (NIH, USA). Antibodies used: anti-mouse Nanog anti-mouse polyclonal antibody (#GTX627421, GeneTex, CA, USA) β-actin rabbit polyclonal antibody (#4970, Cell Signalling Technology, MA), HRP-conjugated anti-rabbit-IgG (Cat no. 7074, Cell Signalling Technology, MA).

2.10 Statistical analysis

Normal distribution (Shapiro–Wilk test) and homogeneity of variances (Brown Forsythe test) were performed. One way ANOVA was used to analyze the results. All statistical analyses were performed with Prism 7 (Graph Pad Software, CA), at a significance level of 5% ($P < 0.05$). Data were represented as mean ± SD.

3. Results

3.1. DPI inhibited the growth of miPS-Huh7cmP cells.

In this study, the miPS-Huh7cmP cells were prepared from miPSCs as the CSC model as summarized in Figure 1A. The resultant miPS-Huh7cmP cells became heterogeneous with GFP^+ and GFP^- phenotypes when cultured in adhesive condition. Passage of the cells was made before 80% confluent so that GFP^+ population was retained to maintain the self-renewal potential for the following experiments. Then, we observed the change in the morphology and fluorescence of GFP to estimate the overall effect of DPI

and VAS2870 on miPS-Huh7cmP cells (Figure 1B). Up to 100 nM of DPI did not show any effect on the miPS-Huh7cmP cells for DPI treated cells. On the other hand, at 1000 and 2000 nM of DPI, the number of both GFP^+ and GFP^- cells appeared to be reduced. At the same time, the cells were treated with VAS2870 up to 2000 nM exhibiting no effect on the morphology and fluorescence at 1000 nM, while the cell density became 70 to 80% at 2000 nM. To confirm this observation, the effect of DPI and VAS2870 were subjected to MTT assay to check the proliferation of the cells (Figure 1C). As the result, the concentration of 50% inhibition (IC_{50}) of DPI in miPS-Huh7cmP cells was estimated to 712 nM, whereas that of VAS2870 could not be estimated. The effect of DPI was further assessed on the cell cycle progression (Figure 2). The cell cycle was not affected in the range of 0 to 100 nM of DPI. However, in 1000 nM, from the comparison of the ratio of each population, G1 and S phases were not apparently affected but G2 phase population had decreased.

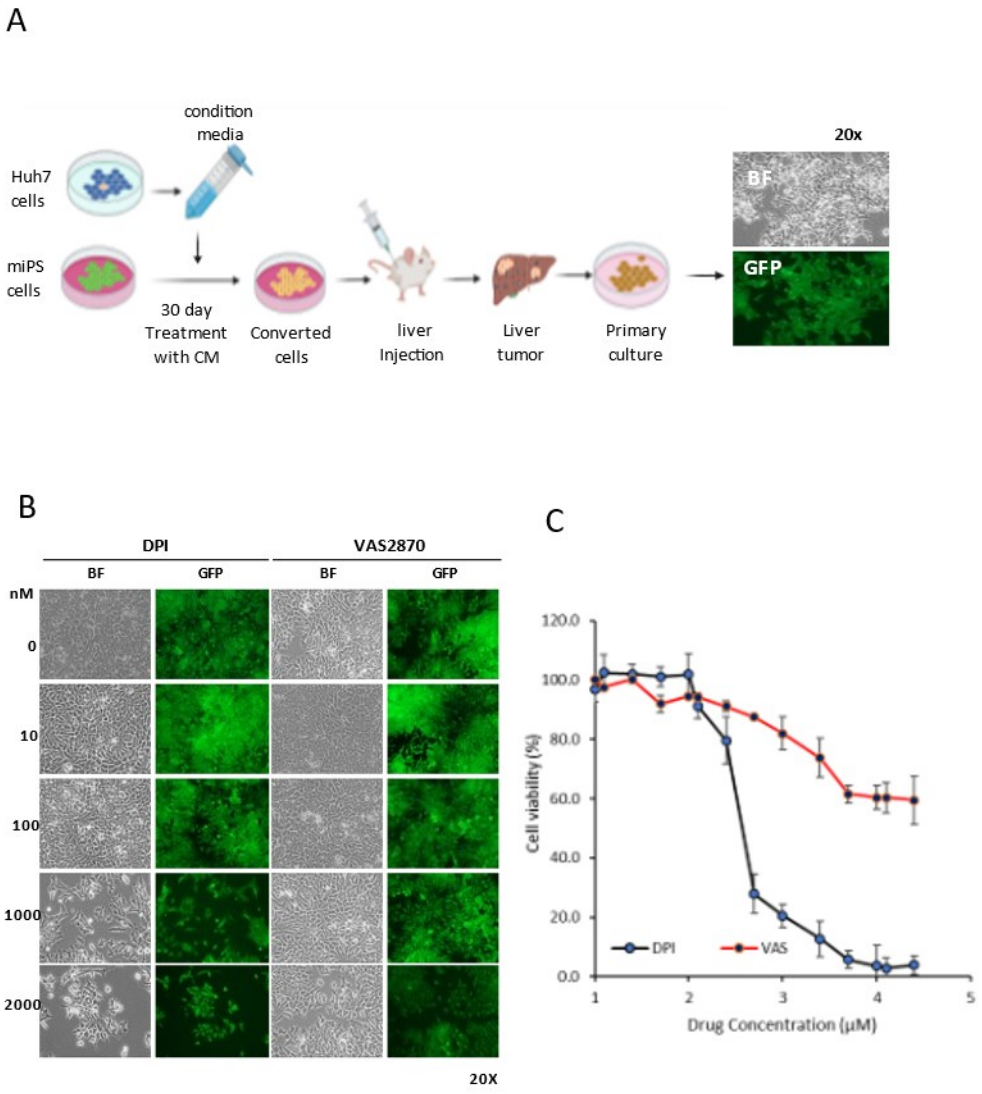

Figure 1. Scheme of preparation of miPS-Huh7cmP cells and the effect of DPI and VAS2870 on cell viability. A, a schematic diagram of the preparation of iPSC derived

CSCs miPS-Huh7cmP cells, which were prepared as the primary culture from the tumor of miPS-Huh7cm cells. B, observation of the cells under bright field and fluorescence of GFP. The cells in the adhesive 2D culture, treated with 0 to 2000 nM of DPI and VAS2870 for 48hrs. C, cell viability was estimated by MTT assay. The value from the cells without DPI was considered as 100%. Each plot was depicted by mean + SD.

3.2. DPI inhibited the self-renewal of miPS-Huh7cmP cells.

We assessed the effect of DPI and VAS2870 on the sphere formation of miPS-Huh7cmP cells. Microscopic observation revealed the sphere formation of the cells was completely inhibited at 500 nM of DPI while VAS2870 up to 1000 nM did not (Figure 3A). The sphere numbers decreased in the presence of DPI in a dose dependent manner in the range of 0 to 1000 nM (Figure 3B). The IC_{50} of DPI was estimated to approximately 5.2 nM. and 500 nM of DPI completely abrogated the sphere formation while VAS2780 did not show any effect. Nanog expression in the presence of DPI and VAS2870 was further assessed by western blotting (Figure 3C). Nanog expression was decreased in a dose dependent manner of DPI in the range of 0 to 2000 nM whereas abrogated at 2000nM while was not affected by VAS2870 (Figure 3D). This result indicated that DPI is directly affecting the pluripotency of the CSCs.

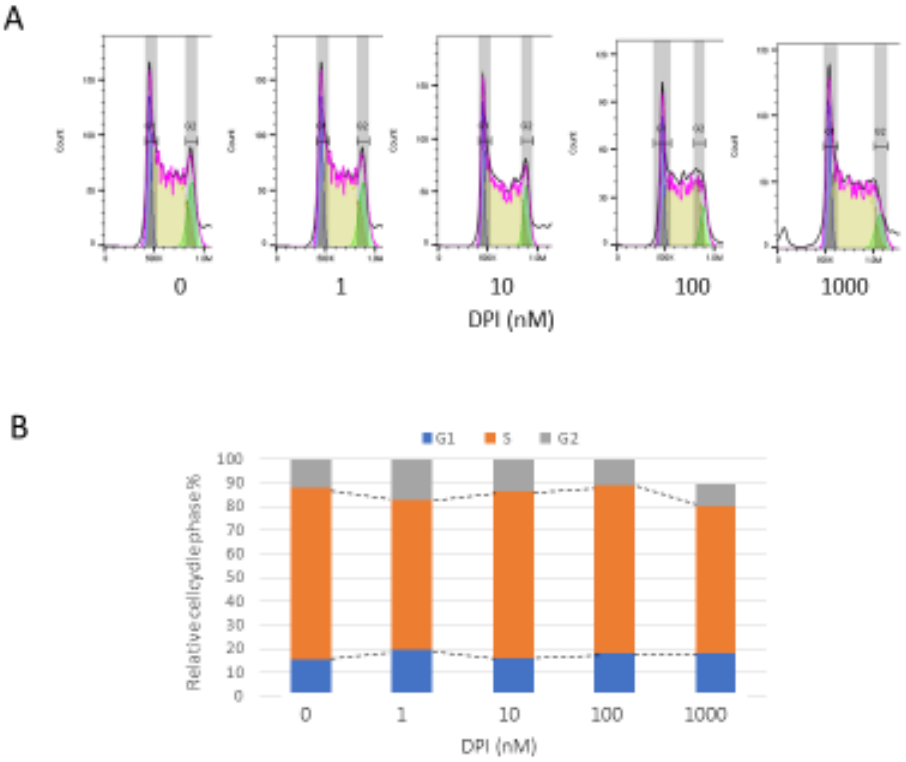

Figure 2. Effect of DPI on the cell cycle of miPS-Huh7cmP cells. A. shows flowcytometric analysis of miPSHuh7cmP cells from adhesive 2D culture treated with various concentration of DPI stained with PI. The peak was analyzed by FlowJo and the horizontal bars depict G1 and G2 phases. B. shows the results of the flowcytometric analyses in A, ratio was calculated and summarized in bar graph, representing different phases of the cell cycle.

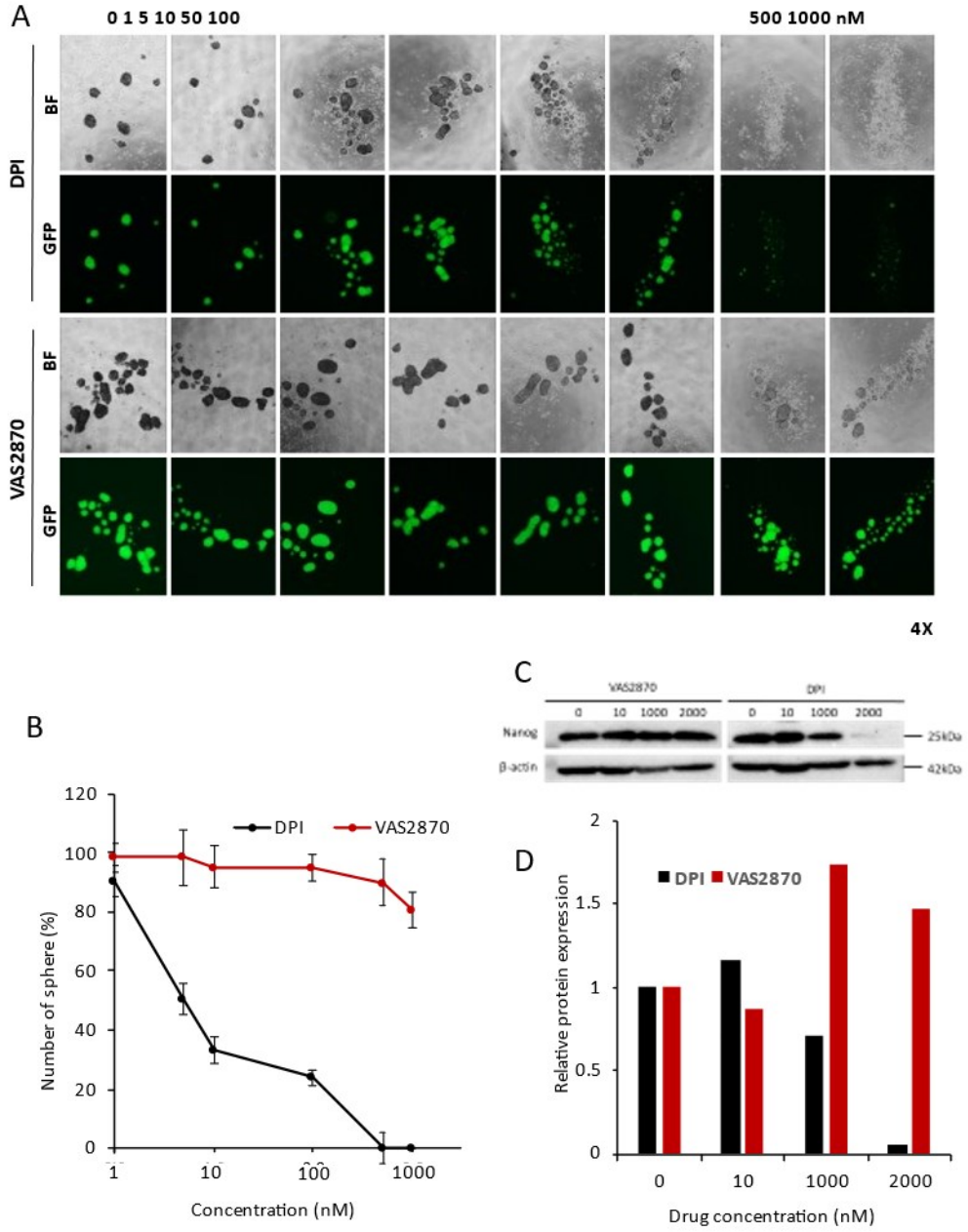

Figure 3. Effect of DPI and VAS2870 on the sphere formation of miPS-Huh7cmP cells. A, sphere formation in 3D culture observed in bright field and fluorescence of GFP in the presence of DPI in 0 -1000 nM. B, change of the percentage of spheres according to

the concentration of DPI and VAS2870. The value from the cells without drug was considered as 100%. Each plot was depicted by mean ± SD. C, Western blot analysis of Nanog upon treatment with DPI and VAS2870. β-actin was used for normalization. D. Integral intensity measurements of the western blot bands shown in (a) normalized to β-actin.

3.3. Effect of DPI on the differentiation of miPS-Huh7cmP cells

We assessed the effect of DPI on the differentiation of miPS-Huh7cmP cells in adhesive 2D culture condition measuring the reduction of GFP population by flow cytometer. DPI at 0 to 500 nM did effect on the differentiation showing almost 93% of the population stably remained GFP^+. However, at the range of 1000 to 2000 nM the GFP^- cells started to increase indicating the differentiation gradually progressed (Figure 4B). DPI at 1000 and 2000 nM increased GFP^- population to 13% and 25%, respectively. The effect of DPI on the differentiation was further assessed on the tube forming assay since mips-Huh7cmP cells were previously shown to differentiate into endothelial like cells on Matrigel (Figure 4C). When the branching points of the tubes were counted, the number was found to be significantly decreased in a dose dependent manner of DPI. On the contrary, the VAS2870 treated cells showed no effect on the number of the branching points of the tubes. From the results the IC_{50} value of DPI was estimated to be 8.7 nM (Figure 4D). To confirm the formed tubes were consisting of CD31 positive endothelial cells were further subjected to the immunofluorescence analysis. As a result, tube like structure was positively stained with anti-CD31 antibody together with GFP showing undifferentiated miPS-Huh7cmP cells and differentiated endothelial

like cells whereas 1000 nM of DPI did not allow the appearance of CD31 positive cells (Figure 4E).

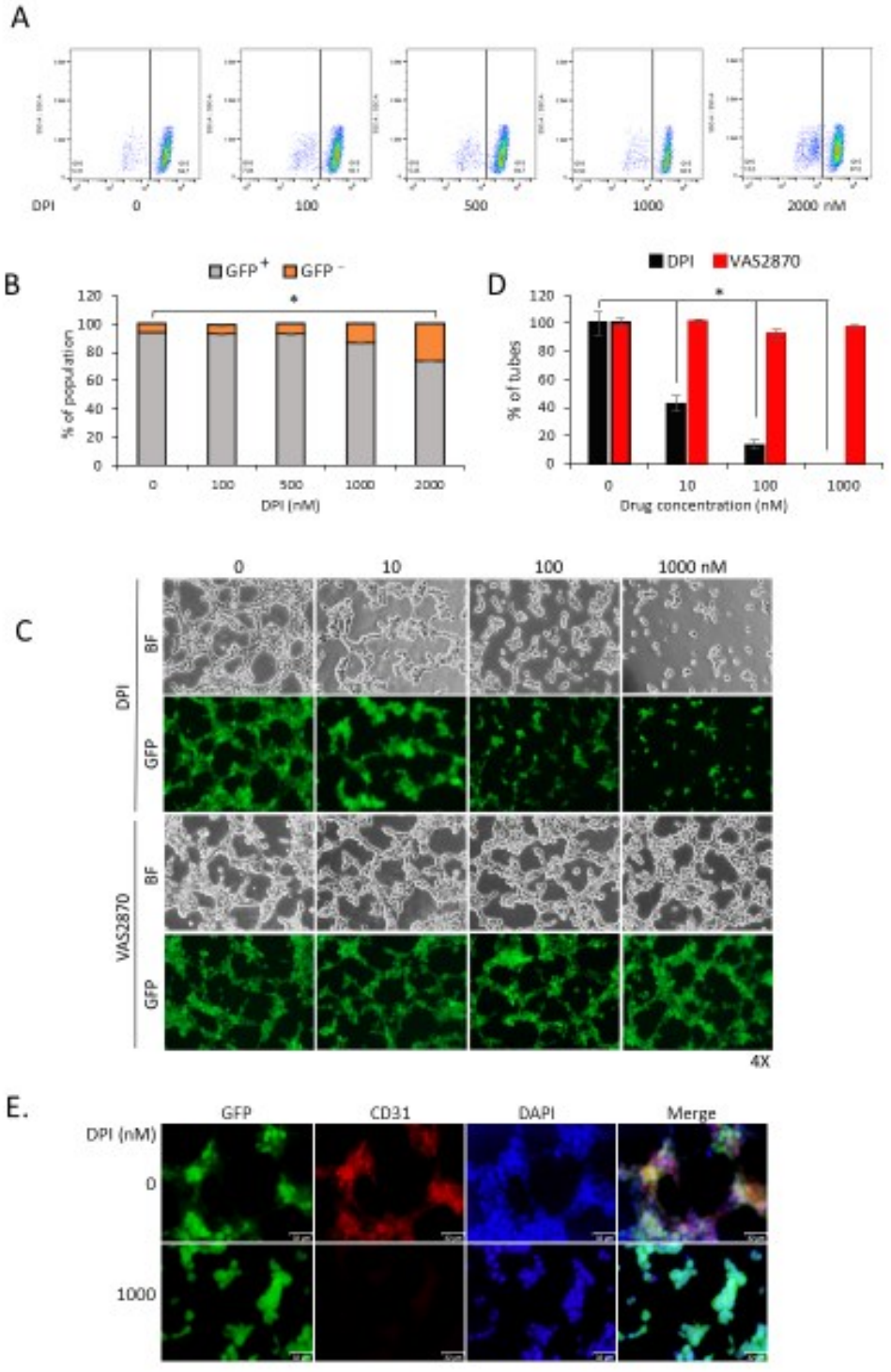

Figure 4. Effect of DPI on the differentiation of miPS-Huh7cmP cells. A, flowcytometric analysis of GEP+ and GFP- population treated with DPI from 0 – 2000 nM. B, bar graphs

representing GFP+ and GFP- population. C, tube formation assay on Matrigel. Cells were seeded in the presence of DPI or VAS2870 in the range of 0 to 1000 nM. BF, bright field. Objective lens 4x. D, bar graphs representing the number of tubes in C as percent to control analysed by ImageJ. E, the immunofluorescence of CD31 together with GFP and DAPI in the tube-like structure. Scale bar = 32 μm. B, D. Each plot was averaged from independent triplicates with S.D. The significance was evaluated by ANOVA where *P ≤ 0.0001.

3.4. Effect of DPI on colony formation and migration ability of miPS-Huh7cmP cells

The effects of DPI and VAS2870 in the range of 0 to 1000 nM on tumorigenic and metastatic characters of miPS-Huh7cm cells *in vitro* were assessed on colony formation and migration (Figure 5A). The colony formation was inhibited in the presence of DPI in a dose dependent manner with the IC_{50} at approximately 12.0 nM In the migration assay, the scratch in dish was monitored for the wound healing in the presence of DPI and VAS2870 for 12 hours, which was shorter than the doubling time of the cells(Figure 5B). The effect of both drugs was apparently monitored from the photographs excluding the possibility of cell division. As the results, DPI was not effective on the migration of the cells in the range of 10 to 100 nM while 1000 nM of DPI significantly decreased the migration while VAS2870 did not show any effect on migration in the range of 0 to 1000 nM. This result indicated the IC_{50} of DPI on the migration should be present between 100 and 1000 nM. If roughly estimated, this

would be approximately 500 nM, which could be correlated with the IC_{50} of growth inhibition at 712 nM.

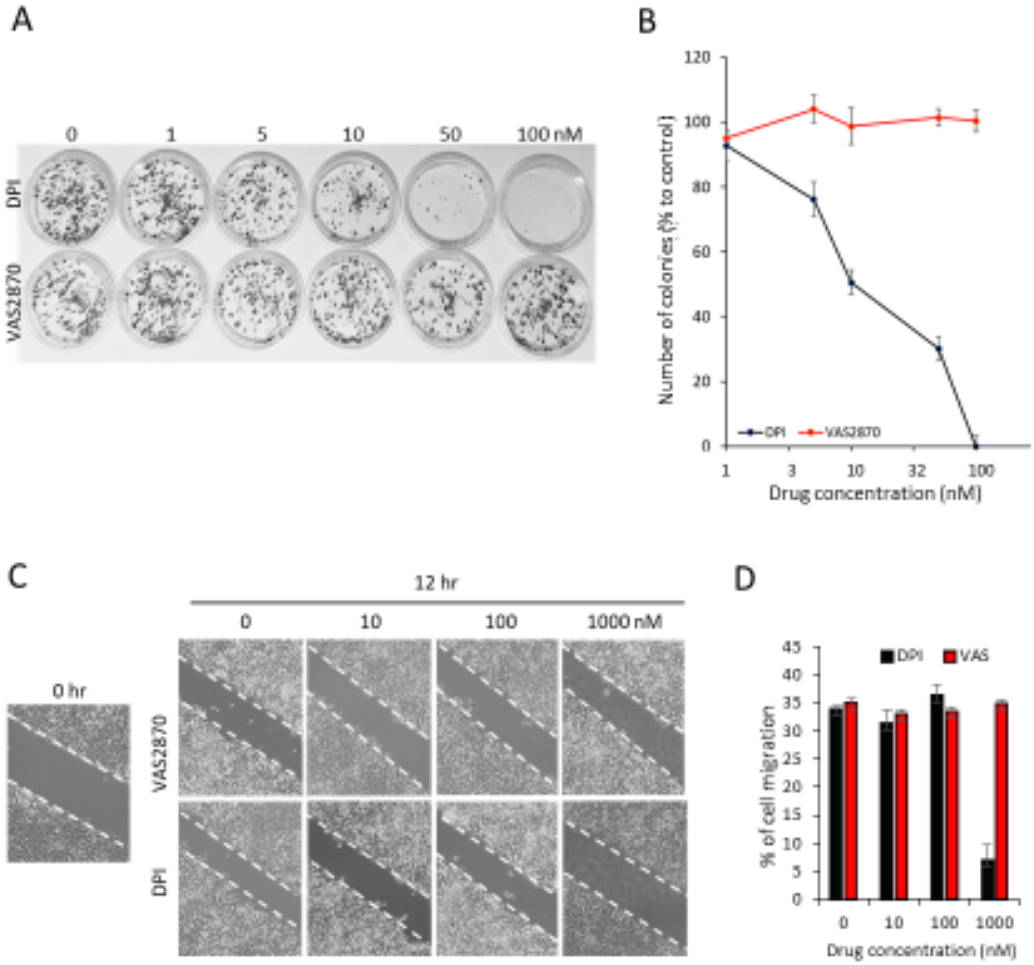

Figure 5. Effect of DPI and VAS2870 on the colony formation and migration of miPS-Huh7cmP cells. A, shows colony formation assay of cells treated with different concentrations of DPI and VAS2870 from 0 - 100 nM. B, percentage of colonies plotted from the results of colony formation assay. C, scratch wound-healing assay in the

presence of DPI and VAS2870 from 0 to 1000 nM. D, percentage of cell migration was measured by ImageJ and depicted in bar graph. Each plot was averaged from independent triplicates with S.D. The significance was evaluated by ANOVA where *P ≤ 0.0001.

4. Discussion

In this study the effect of DPI was assessed on a cancer stem cell model of miPS-Huh7cmP cells, which was established as a liver cancer stem cell model from mouse iPSCs. In this model, stemness was visualized as GFP^+ subpopulation while the differentiated cells resided as GFP^- subpopulation (Figure 1A). This heterogeneity of the population is generally common with the cancer tissues. It is considered as the results of self-renewal and differentiation of CSCs, which could be mimicked by the miPS-Huh7cmP cells. With the heterogeneity, the IC_{50} values of functional assays upon drug treatment might be mixed depending on the subpopulations. This would be the reason why the IC_{50} values were apparently high in the adhesive culture that contains both differentiated and undifferentiated subpopulations. This heterogeneity could be reconstituted either in the monolayer of 2D culture condition or extracellular matrix assisted and/or 3D culture condition. Currently, the 3D culture condition is considered more natural compared to the 2D condition, which means that 3D condition could be the more practical way of assessment [16,17]. In this study, 2D culture condition was exploited for the assays on cell growth, cell cycle and scratch, whereas the IC_{50} values of DPI on miPS-Huh7cmP cells were ranging between 100 and 1000 nM. From these results, miPS-Huh7cmP cells appeared rather insensitive to DPI. These values of DPI

were similar with the those of previous studies on the human retinal pigment epithelium cell line ARPE-19 cells[18]. Clonogenic assay or colony formation assay is an *in vitro* cell survival assay based on the ability of a single cell to grow into a colony in 3D[19,20]. On the contrary to the 2D condition, the assays in 3D condition, such as sphere, colony, and tube formation, gave IC_{50} ranging in 5 to 12 nM, which are clearly lower than those observed in the 2D condition. DPI inhibited the self-renewal ability of miPS-Huh7cmP cells at the IC_{50} of 5.2 nM (Figure 3), the differentiation at the IC_{50} of 9 nM (Figure 4C, D), and the colony formation at the IC_{50} of 12 nM (Figure 5A, B). In contrast, VAS2870 did not inhibit the CSC characteristics assessed in this study. This could be explained by the difference of specificity of DPI and VAS2870. DPI is an inhibitor that binds the flavin adenine dinucleotide (FAD)- and flavin mononucleotide (FMN)-binding domains of succinate dehydrogenase in the mitochondrial complex II, NADPH oxidases, xanthine oxidase and nitric oxide synthase. On the other hand, VAS2870 binds to the FAD- and FMN-binding domains via thioalkylation of cysteine residues, so that the binding should be limited to those with cysteine residue. Taking these into consideration, the anti-CSC effect of DPI demonstrated in this study appears due to the inhibition of the enzymes with the domains lacking the cysteine residues [21,22]**.** In this context, our results indicated the presence of enzymes, which is related with mitochondrial respiration described below, and by which DPI inhibited but VAS2870 did not, although further investigation is still required. The IC_{50} of DPI as 10nM was described in the 3D culture conditions of murine neural stem cells[23]. Also, DPI inhibited mitochondrial respiration at 10 nM reducing the oxidative ATP production in the

mammosphere of CSCs derived from human breast cancer cell line MCF7 cells[22]. The 3D condition represents and mimics the natural conformation of tumors and its surrounding microenvironment allowing the CSCs to grow in spheres. The concentration from the previous reports is consistent with our current study demonstrating DPI inhibited the self-renewal of CSCs as well as the differentiation. Although, results of the inhibition of both self-renewal and differentiation at the same time appear contradictory, it is worthwhile noticing that the tube formation demonstrated the presence of both phenotypes coexisted in the same structure as shown in Figure 4E. As we previously demonstrated, CSCs became heterogeneous in the culture and the differentiated phenotype of the cells supported the self-renewal potential of CSCs by enhancing the sphere formation[24]. Since the 3D culture condition represents and mimics the natural conformation of tumors and its surrounding microenvironment allowing the CSCs to grow in spheres, 3D culture technique could be preferable for drug screening against CSCs. At the same time, we suggest that DPI would be a favorable candidate to treat CSCs.

5. Conclusions

DPI inhibited the three major characteristics, self-renewal, differentiation, and tumorigenic potential with malignancy, of miPS-Huh7cmP cells as a cancer stem cell model. Since this was found only in the 3D related culture conditions, we suggest that the screening of anti-CSC molecules should be performed under 3D conditions. Taking the character of DPI mitochondrial respiration was confirmed as a good target of cancer stem cells.

References

1. Chen L, Kasai T, Li Y, et al. A model of cancer stem cells derived from mouse induced pluripotent stem cells. PLoS One. 2012;7(4):e33544.

2. Afify SM, Seno M. Conversion of Stem Cells to Cancer Stem Cells: Undercurrent of Cancer Initiation. Cancers (Basel). 2019;11(3).

3. Nawara HM, S MA, Hassan G, et al. Paclitaxel and Sorafenib: The Effective Combination of Suppressing the Self-Renewal of Cancer Stem Cells. Cancers (Basel). 2020;12(6).

4. Seno A, Mizutani A, Aizawa K, et al. Daunorubicin can eliminate iPS-derived cancer stem cells via ICAD/CAD-independent DNA fragmentation. Cancer Drug Resistance. 2019;2(2):335-350.

5. Fong D, Christensen CT, Chan MM. Targeting Cancer Stem Cells with Repurposed Drugs to Improve Current Therapies. Recent Pat Anticancer Drug Discov. 2021.

6. Nawara HM, Afify SM, Hassan G, Zahra MH, Seno A, Seno M. Paclitaxel-Based Chemotherapy Targeting Cancer Stem Cells from Mono- to Combination Therapy. Biomedicines. 2021;9(5).

7. Bose S, Zhang C, Le A. Glucose Metabolism in Cancer: The Warburg Effect and Beyond. Adv Exp Med Biol. 2021;1311:3-15.

8. Bergers G, Fendt SM. The metabolism of cancer cells during metastasis. Nat Rev Cancer. 2021;21(3):162-180.

9. Kahlert UD, Mooney SM, Natsumeda M, Steiger HJ, Maciaczyk J. Targeting cancer stem-like cells in glioblastoma and colorectal cancer through metabolic pathways. Int J Cancer. 2017;140(1):10-22.

10. Mortezaee K. Redox tolerance and metabolic reprogramming in solid tumors. Cell Biol Int. 2021;45(2):273-286.

11. Pacini N, Borziani F. Cancer stem cell theory and the warburg effect, two sides of the same coin? Int J Mol Sci. 2014;15(5):8893-8930.

12. Piszczatowska K, Przybylska D, Sikora E, Mosieniak G. Inhibition of NADPH Oxidases Activity by Diphenyleneiodonium Chloride as a Mechanism of Senescence Induction in Human Cancer Cells. Antioxidants (Basel). 2020;9(12).

13. Nawara HM, M Afify S, Hassan G, et al. Paclitaxel and sorafenib: The effective combination of suppressing the self-renewal of cancer stem cells. 2020;12(6):1360.

14. Afify SM, Chen L, Yan T, et al. Method to Convert Stem Cells into Cancer Stem Cells. Methods Protoc. 2019;2(3).

15. Pozarowski P, Darzynkiewicz Z. Analysis of Cell Cycle by Flow Cytometry. In: Schönthal AH, ed. Checkpoint Controls and Cancer: Volume 2: Activation and Regulation Protocols. Totowa, NJ: Humana Press; 2004:301-311.

16. Bielecka ZF, Maliszewska-Olejniczak K, Safir IJ, Szczylik C, Czarnecka AM. Three-dimensional cell culture model utilization in cancer stem cell research. Biol Rev Camb Philos Soc. 2017;92(3):1505-1520.

17. Hassan G, Afify SM, Kitano S, et al. Cancer Stem Cell Microenvironment Models with Biomaterial Scaffolds In Vitro. 2021;9(1):45.

18. Park SE, Song JD, Kim KM, et al. Diphenyleneiodonium induces ROS-independent p53 expression and apoptosis in human RPE cells. FEBS Lett. 2007;581(2):180-186.

19. Beck B, Blanpain C. Unravelling cancer stem cell potential. Nat Rev Cancer. 2013;13(10):727-738.

20. Rajendran V, Jain MV. In Vitro Tumorigenic Assay: Colony Forming Assay for Cancer Stem Cells. Methods Mol Biol. 2018;1692:89-95.

21. Altenhöfer S, Kleikers PW, Radermacher KA, et al. The NOX toolbox: validating the role of NADPH oxidases in physiology and disease. 2012;69(14):2327-2343.

22. Ozsvari B, Bonuccelli G, Sanchez-Alvarez R, Foster R, Sotgia F, Lisanti MPJA. Targeting flavin-containing enzymes eliminates cancer stem cells (CSCs), by inhibiting mitochondrial respiration: Vitamin B2 (Riboflavin) in cancer therapy. 2017;9(12):2610.

23. Haigh CL, Tumpach C, Collins SJ, Drew SC. A 2-Substituted 8-Hydroxyquinoline Stimulates Neural Stem Cell Proliferation by Modulating ROS Signalling. Cell Biochem Biophys. 2016;74(3):297-306.

24. Matsuda S, Yan T, Mizutani A, et al. Cancer stem cells maintain a hierarchy of differentiation by creating their niche. 2014;135(1):27-36.

Chapter 4: Modelling of Glioblastoma stem cells from miPS cells

Abstract.

Glioblastoma Multiforme is the deadliest tumor with a median survival of 15 months. Glioblastoma stem cells or brain tumor propagating cells have recently gained immense attention. We tried to establish Glioblastoma stem cells (GCSs) from miPS cells using condition media from different glioblastoma cell lines A172, GI1, U251MG. The miPSCs treated with CM exhibited self-renewal and differential potential in vitro. The cells were injected subcutaneously in BALB/c nude mice formed malignant tumors. The primary cells derived from the malignant tumor also possessed self-renewal capacity and differentiation potential and expressed CSC and GMB associated markers. We conclude that using condition media from malignant glioblastoma cell lines can efficiently mimic the tumor microenvironment that can convert miPSs to GSCs. This approach could be a novel method for in vitro disease modeling Glioblastoma Multiformie to elucidate underlying molecular mechanisms for brain-related malignancies.

Introduction

Glioblastoma is a universally lethal disease with no effective therapy. The current standard of care for glioblastoma patients includes maximal surgical resection, concurrent radiotherapy, and treatment with alkylating agent temozolomide, followed by adjuvant temozolomide. This treatment regimen extends survival to a median of only 14.6 months. Glioblastomas are complex ecosystems that rapidly evolve in response to harsh environmental conditions. Recent evidence shows that the intratumoral heterogeneity and therapy resistance that characterize glioblastomas are promoted by glioblastoma stem cells (GSCs). These GSSs portray features of stem cells such as self-renewal, differentiation, pluripotency, and tumorigenicity that drive resistance to pharmacology, radiation, and surgery. For these reasons, the GSCs are now considered a critical therapeutic target. It is evident that the GSCs can thrive in harsh, complex microenvironmental niches and are uninfluenced by stringent checkpoints on proliferation and survival that stringent their regular counterparts. However, the number of GSCs is low in the tumor, and the isolation is challenging. In this study, we attempted to experimentally produce GSCs from induced pluripotent stem cells (iPSCs) using conditioned media (CM) from different glioblastoma cell lines-

that occasionally secrete several different autocrine or paracrine factors which mimic tumor microenvironment that stimulates cells to initiate carcinogenesis.

In this study

In this study we used cells lines A172, U251MG and GI1 to harvest condition media and then treat the miPS cells for 3 weeks to check if neuronal differentiation was visible and if the cells were showing characteristics of GSCs.

Aim of the Study

The aim of the study was to produce Glioblastoma stem cell model from miPS cells. Then use the GSCs to evaluate the efficacy of DPI using different 2D and 3D cell culture techniques.

Material and methods

2.1 Cell culture

Human HCC cell line A172 and U251MG (Riken Cell Bank, Japan) was cultured in Dulbecco's Modified Eagle's Medium (DMEM, Sigma-Aldrich, USA) supplied with 10% foetal bovine serum (FBS) and 100 U/mL penicillin/streptomycin (Wako, Japan). The cells were incubated in a 37 °C incubator with 5% CO_2. When the cells reached 80% confluence, The medium was changed to 5% FBS and then the cells were incubated for 48 hours. After 48hrs the medium, also referred to as condition media (CM) from the cell culture were harvested, centrifuged for 10 min at 1000 rpm at room temperature and then filtered through a 0.22 µm filter (Millipore, Ireland). Mouse iPSCs (miPSCs) were maintained under the humidified 5% CO_2 atmosphere at 37 °C on feeder layer of mitomycin-C-treated mouse embryonic fibroblasts (Reprocell, Japan) in miPS medium

(DMEM containing 15% FBS, 0.1 mM non-essential amino acid (NEAA), Thermo Fisher Scientific, USA), 2 mM L-Glutamine (Nacalai Tesque, Japan), 0.1 mM 2-mercaptoethanol (Sigma-Aldrich, USA), 1000 U/mL leukaemia inhibitory factor (LIF) (Merck Millipore, USA) and 100 U/mL penicillin/streptomycin (Wako, Japan). After 1 week, miPSCs were transferred to gelatine (Sigma-Aldrich, USA) coated dishes. After 70% confluence, miPSC conversion was started using 1:1 ratio of miPS medium and CM from A172, U251MG and GI1 cells for 4 weeks. The converted cells established from miPSCs in the CM for 4 weeks were named as miPS-A172cm, miPS-U251MGcm and miPS-GI1cm cells. Nanog-GFP reporter expression was used in miPSCs and the expression of green fluorescent protein (GFP) reflects the maintenance of stemness. For primary culture, tumour tissues were cut into small pieces in PBS. Then these were suspended into a 15-ml tube containing dissociation buffer (0.25% trypsin) and incubated at 37 °C for 1 h. After digestion, the suspension was mixed well using 1 ml pipette. Then the mixture was incubated for 5 min at 37°C until large pieces broken down. The supernatant was transferred to a new tube containing 1 ml 10% FBS medium to stop digestion. The cellular suspension was centrifuged at 300 rpm for 3 min, and then the supernatant was transferred again to a new tube that was centrifuged at 1000 rpm for 10 min. The cell pellet was then placed in an appropriate volume of miPS medium without LIF, and the cells were seeded into a dish at a density of 1×10^5/ml. These primary cells were named as miPS-A172cmP and miPS-U251MGcmp cells. Cell morphology was observed and photographed using Olympus IX81 microscope equipped with a light fluorescence device (Olympus, Japan).

2.2 Tumorigenicity assay in vivo

To explore the tumorigenic capacity, 4-week-old Balb/c-nu/nu female immunodeficient mice (3 mice for each cell line; Charles River, Japan) were euthanized with 2% isoflurane through inhalation and 1×10^6 cells suspended in 50 µL HBSS (Gibco, Japan) and injected subcutaneously. Tumor growth was monitored weekly after implantation. After three weeks, animals were sacrificed by euthanasia with 5% of isoflurane through inhalation to ensure rapid loss of consciousness and cardiac arrest followed by cervical dislocation to confirm the death of mice. The plan of animal experiments was reviewed and approved by the ethics committee for animal experiments of Okayama University under the IDs OKU-2013252 and OKU-2016078. All animal experiments have been performed in accordance with the ARRIVE/NC3R guidelines.

2.3 Sphere formation assay

Cells were seeded at a density of $4x10^4$ cells/well in 12-well ultralow attachment plates (Corning Inc., NY) in sphere-forming media (DMEM supplemented with 1% v/v insulin-transferrin-selenium-ethanol (ITS-x) (Wako-Fujifilm, Japan), 1 mM l-glutamine, 0.1 mM NEAA, 0.1 mM beta-mercaptoethanol, 0.5 U/ml penicillin/streptomycin). After five days, images were captured using an inverted fluorescence microscope (IX81, Olympus, Japan).

2.4 In vitro tube-formation assay

Cells, 5 × 10^5 cells, were collected, resuspended in endothelial basal medium EBM2 media (EBM-2 Single Quots Kit, Lonza, Switzerland), and seeded in 12-well plates coated with growth factor-reduced Matrigel (Corning Inc., Corning, USA) for 24 h in the presence ascorbic acid (1 μg/ml), human basic fibroblast growth factor (FGF; 10 ng/ml), heparin (22.5 μg/ml) and FBS (0.02 mL/ml). Experiments were performed in triplicate. Images of formed tubes were captured by the Olympus IX81 microscope (Olympus, Japan).

2.5 Immunofluorescence

For immunofluorescence analysis, after incubation, cells were washed with PBS, fixed with 4% paraformaldehyde for 20 min at room temperature, and subsequently permeabilized with 100% methanol. The cells were incubated in blocking solution (PBS supplemented with 10% FBS) for 1 hr followed by incubation overnight at 4°C with the primary antibody. Then cells were washed and incubated with the secondary antibody. After removing and washing the secondary antibody, nuclei were counterstained with 4, 6-diamino-3-phenylidole dihydrochloride (Sigma-Aldrich, USA) and mounted on glass slides using Vecta-shield mounting medium (Vector Labs, USA). Images were taken by Olympus IX81 inverted microscope.

2.6 Histological analysis

Haematoxylin and eosin staining

Tumors were fixed in 10% formalin (Wako Japan), embedded in paraffin wax, and sectioned for histologic examination at five μm. Sections were stained with

hematoxylin 0.5% (Sigma-Aldrich, USA) and eosin Y (Sigma-Aldrich, USA). Slides were analyzed using a light microscope (Eclipse Ti, Japan).

Immunohistochemistry (IHC)

IHC performed was the same as standard procedures using the ABC reagent (Vector Laboratories, USA). Detection was accomplished using DAB substrates (Vector Laboratories, USA). Incubation of sections with PBS served as the negative control. Sections were lightly counterstained with hematoxylin and mounted with Micro mount (Leica Camera AG, Wetzlar, Germany).

Results.

We tried to establish miPS cell-derived Glioblastoma stem cells (GCSs) using condition media from different cancer cell lines A172 and U251MG. In the 2D culture condition, both cells exhibited two different types of populations; one was colony-expressing GFP, and the other was neuron-like cells attached to the bottom of the dish without expressing GFP. The cells portrayed axon, axon hillock, dendrite, dendritic branches, and telodendrion and synaptic terminals. Based on these features, we tried to assess if the mips-A172cm and miPS-U251MGcm cells were expressing neuronal markers. We stained the cells with NESTIN and Neurofilament-2. The immunofluorescence results indicate that the miPS-A172cm and miPS-U251MG cells are positive for NESTIN and Neurofilament-2. In both types of cells, NF2 is expression is more potent than NESTIN

(Figure 1B). Next, the self-renewal capacity of miPS-A172cm and U251MGcm was assessed.

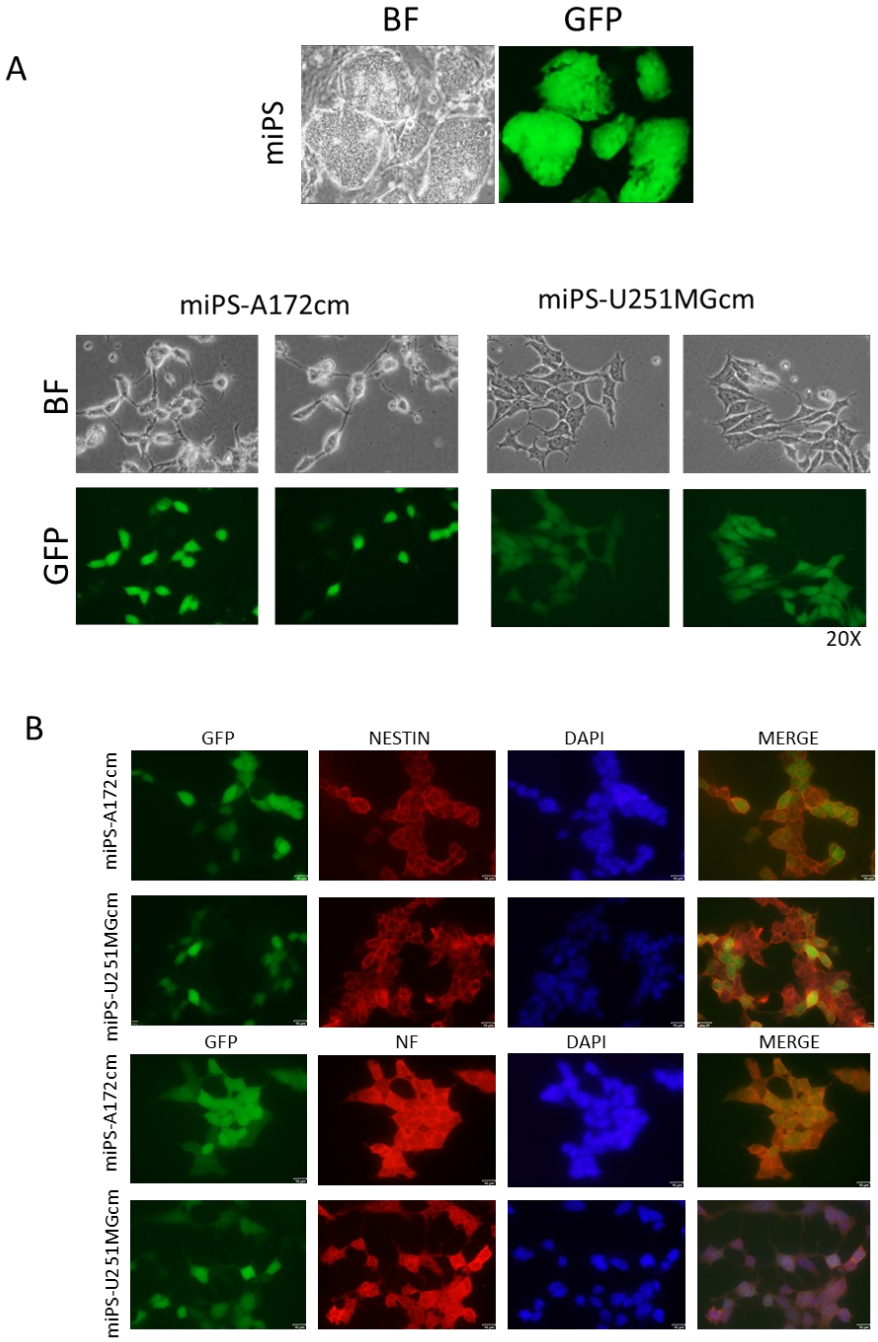

Figure 1: A. the miPS cells and condition media treated miPS cells after 3 weeks. The cells showing neuronal cell like features. B.The cells are positive for Glioblastoma stem cell markers NESTIN and Neurofilament.

In the 2D culture condition, both cells exhibited two different types of populations; one was colony-expressing GFP, and the other was neuron-like cells attached to the bottom of the dish without expressing GFP. The undifferentiated GFP-positive cells were recognized as a neuro-sphere-forming population. miPS-A172cm cells showed significantly high spheroid-forming potential when compared to miPS-U251MGcm cells. This indicated that both cells had self-renewal capacity. To further confirm if the cells were maintaining stemness, we stained with SOX2 antibody, and both miPS-A172cm and miPS-U251MGcm cells were found to be positive for the SOX2, a persistent marker for multipotential neural stem cells (Figure 2).

Differentiation potential is another property of CSCs. We tried to assess the differential potential of miPS-A172cm and miPS-U251MGcm to see if they can differentiate into endothelial-like cells that form capillary-like tube structures on Matrigel. Upon culturing them on Matrigel, these cells confirmed the formation of capillary-like tubes, indicating pro-angiogenic properties of miPS-A172cm and miPS-U251MGcm (Figure 3).

Since the results implied the possible role of miPS-A172cm and miPS-U251MGcm cells in tumor angiogenesis, platelet-endothelial cell adhesion molecule-1 (CD31) expression was evaluated in both cells the cells were found to be positive for the CD31 marker.

miPS-A172cm cells showed significant elevation in the number of branching points per field compared to miPS-U251MGcm.

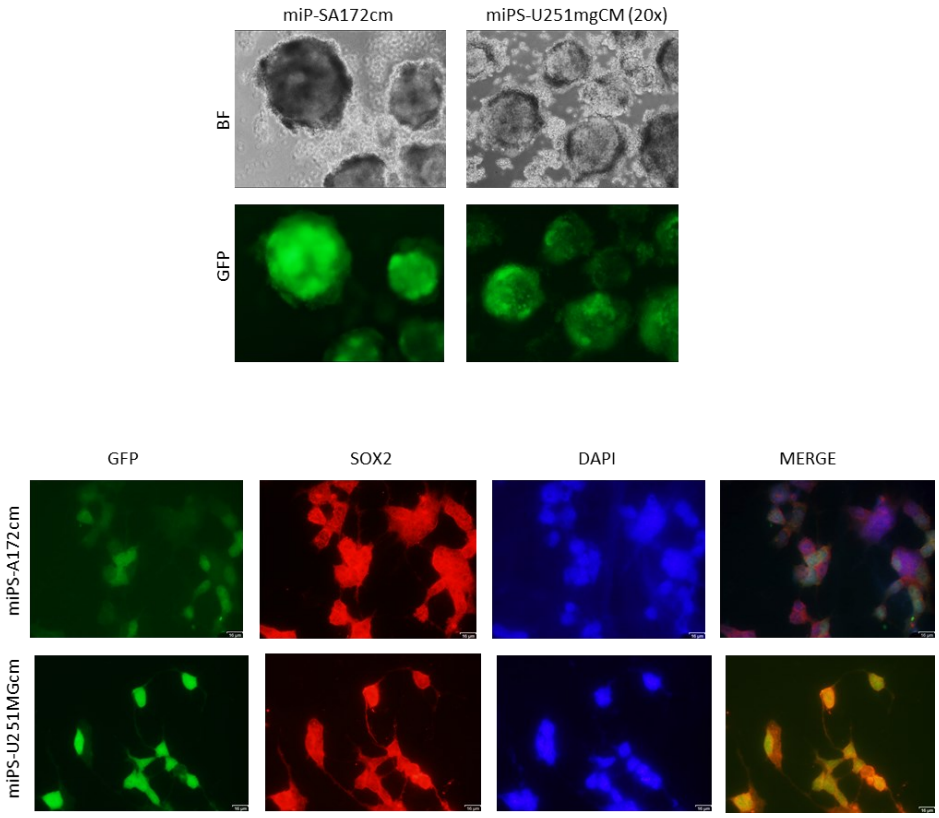

Figure 2. miPS-A172cm and miPS-U251MGcm cells form neuro spheres and the cells are positive for SOX2.

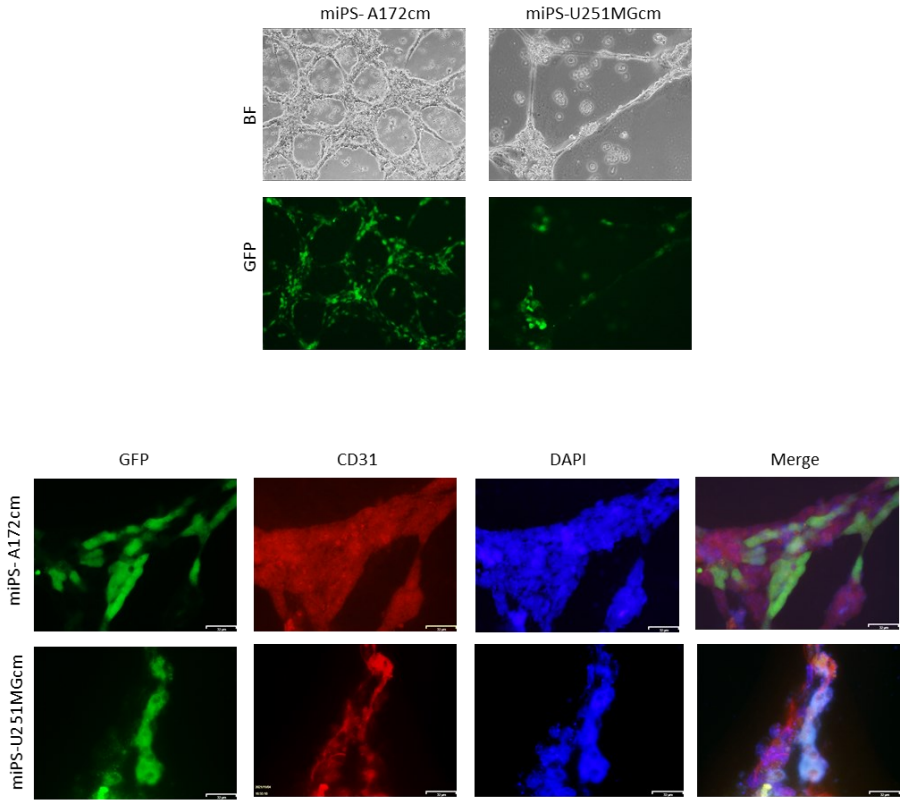

Figure 3. miPS-A172cm and miPS-U251MGcm cells form tube like structures in presence of Matigel. Both miPS-A1722cm and miPS-U251MGcm cells are positive CD31 markers.

To assess the tumorigenic ability of miPS-A172cm and miPS-U251MGcm cells, we checked the tumorigenicity in vivo. Approximately $1x10^6$ cells were subcutaneously injected into three immunodeficient BALB c nu/nu mice. After two weeks of injection, the tumor started to appear. For both injected cells, miPS-A172cmP and miPS-U251MGcm cells grew deep into the injection site, invaded adjacent tissue, and were highly vascularized, 4weeks after injection miPS-A172cm and miPS-U251MGcm developed tumors in all mice. The size of tumors derived from miPS-U251MGcmP cells was significantly higher than that of miPS-A172CM cells, indicating fast growth of tumors derived from miPS-U251MGcm cells were more proliferative and aggressive. Histology of miPS-A172cm and miPS-U251MGcm cell-derived tumors showed that a substantial portion of the tumours expressed a malignant phenotype such as high nuclear-to-cytoplasmic ratio and mitotic figures. Simultaneously, IHC of the tumors showed high SOX2, NF-2, NESTIN, and GFP. Tumors were excised and partly cultured on the gelatine-coated dish in miPS medium to obtain the primary culture (Figure 4).

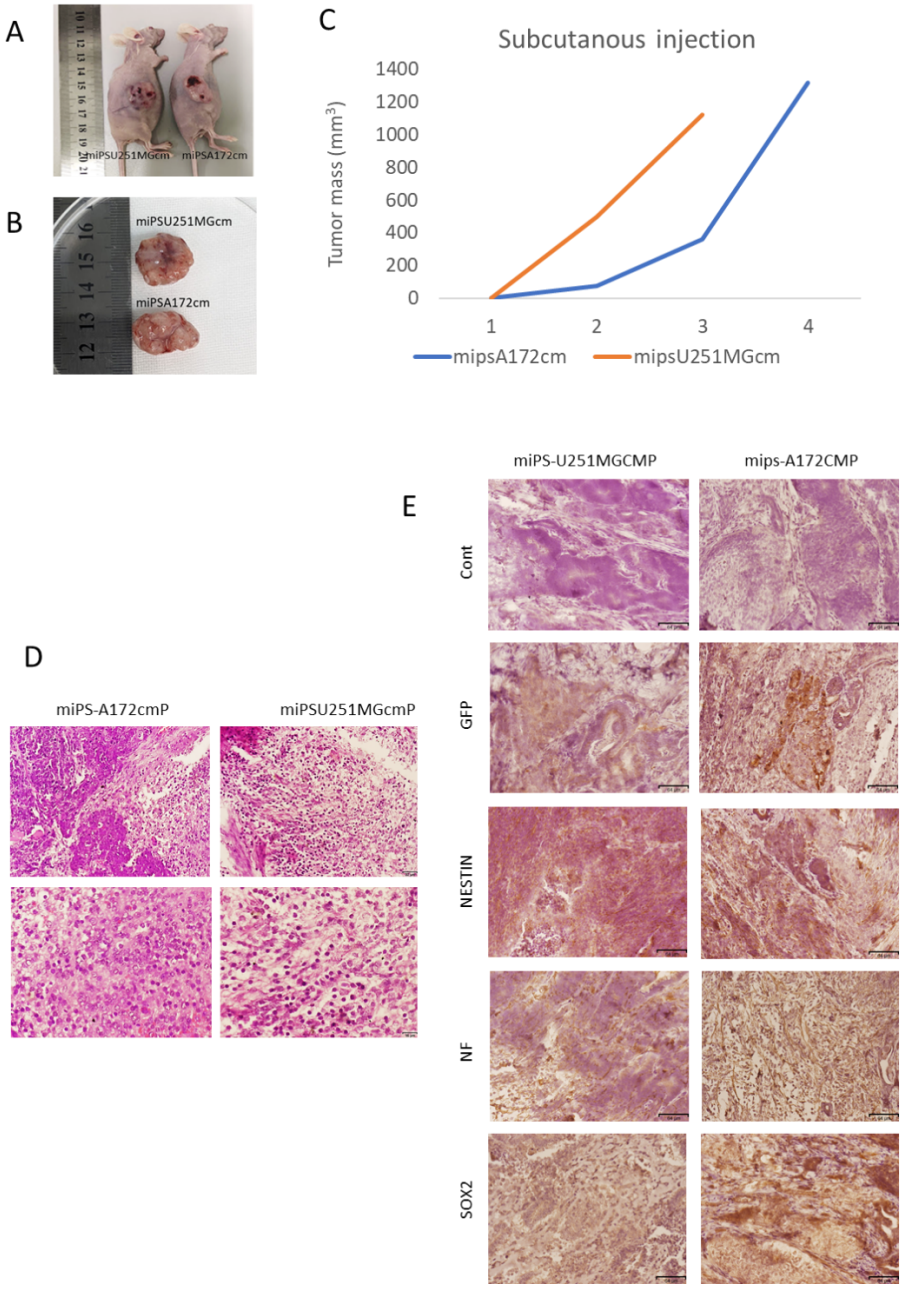

Figure 4. Malignant tumorigenicity of the miPS-A172cmP and miPS-U251MGcmP cells. A. Tumor baring Mouse. B. Tumor harvested from After 3 weeks from nude mice. C. Growth curve representing bulk tumor mass. D. Hematoxylin and eosin staining of tumor sections from tumors caused by miPS-A172cm and miPS-U251MGcm cells showing the presence of mitotic figures. E. Immunohistochemical staining of formalin-

fixed paraffin-embedded tumor tissue. Samples representative of each tumor were stained with antibodies recognizing SOX2, NF-2, GFP and NESTIN. All data were from three independent experiments (n = 3). Scale bars represent 64 µm.

From the primary culture, which exhibited GFP-expressing colonies surrounded by the progenies of neuronal-like cells, GFP expressing puromycin-resistant cells were selected and named as miPS-A172cmP and miPS-U251MGcmP cells. The primary culture from the tumors and primary cells miPS-A172cmP and mips-U251MGcmP also exhibited glioblastoma stem cell markers CD133 and CD144 (Figure 5). At the same time when they were put under 3D culture conditions, the cells showed spheroid-like structures. The primary cells were also positive for SOX2 and formed tube-like structures in Matrigel, showing endothelial differentiation. Since the cells were positive for expressing CSC markers, we tried to assess if the primary (Figure 6 and 7).

We stained the cells with Nf-2, GFAP, and NESTIN to check if the cells were still expressing Neural markers. The results dictated that both primary cells miPS-A172cmP and mips-U251MGcmP were positive for expression of these makers through immunofluorescence (Figure 8).

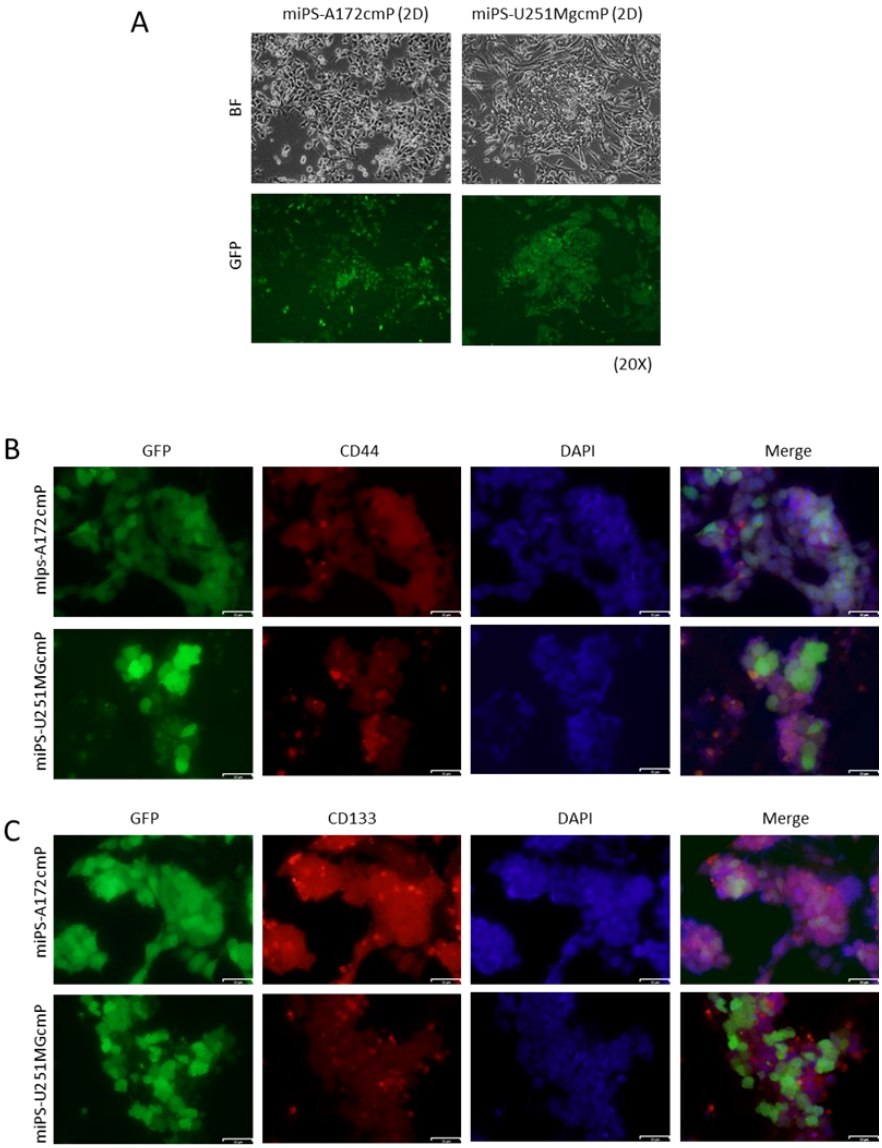

Figure 5. The primary cells obtained from the tumors of the miPSA172cm and U251MGcm cells shows in Figure 3A under 2D condition. Figure 3B and 3C show ICC staining for CD44 and CD133 antibodies.

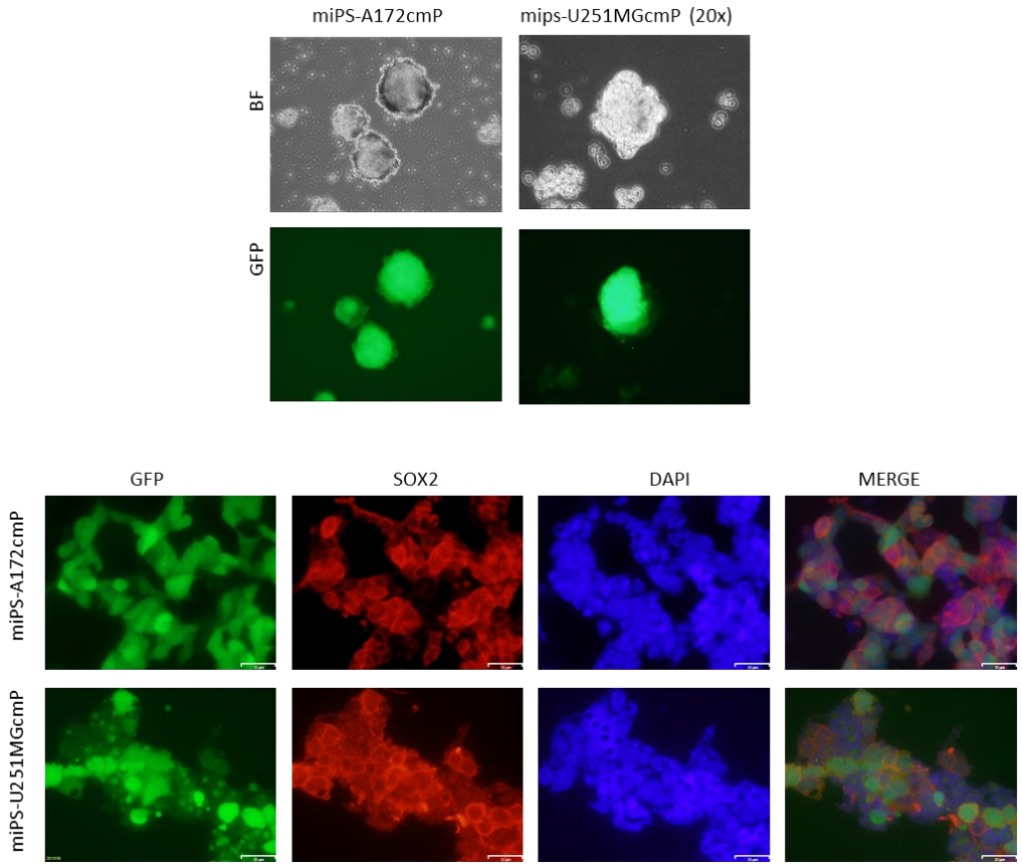

Figure 6: A. miPS A172cmP and miPSU251MGcmP cells forming spheres in vitro. B. the cells forming tubes in vitro. Both of the cells are positive for SOX2 antibody

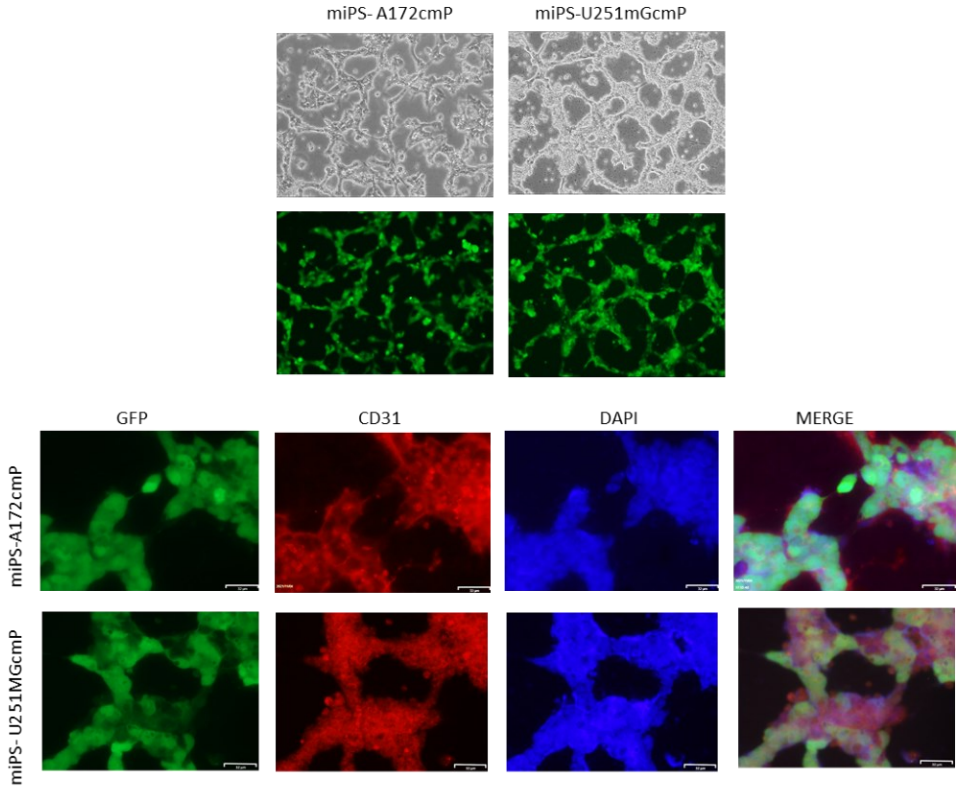

Figure 7: A. miPS A172cmP and miPSU251MGcmP cells forming spheres in vitro. B. the cells forming tubes in vitro. Both of the cells are positive CD31 Antibodies.

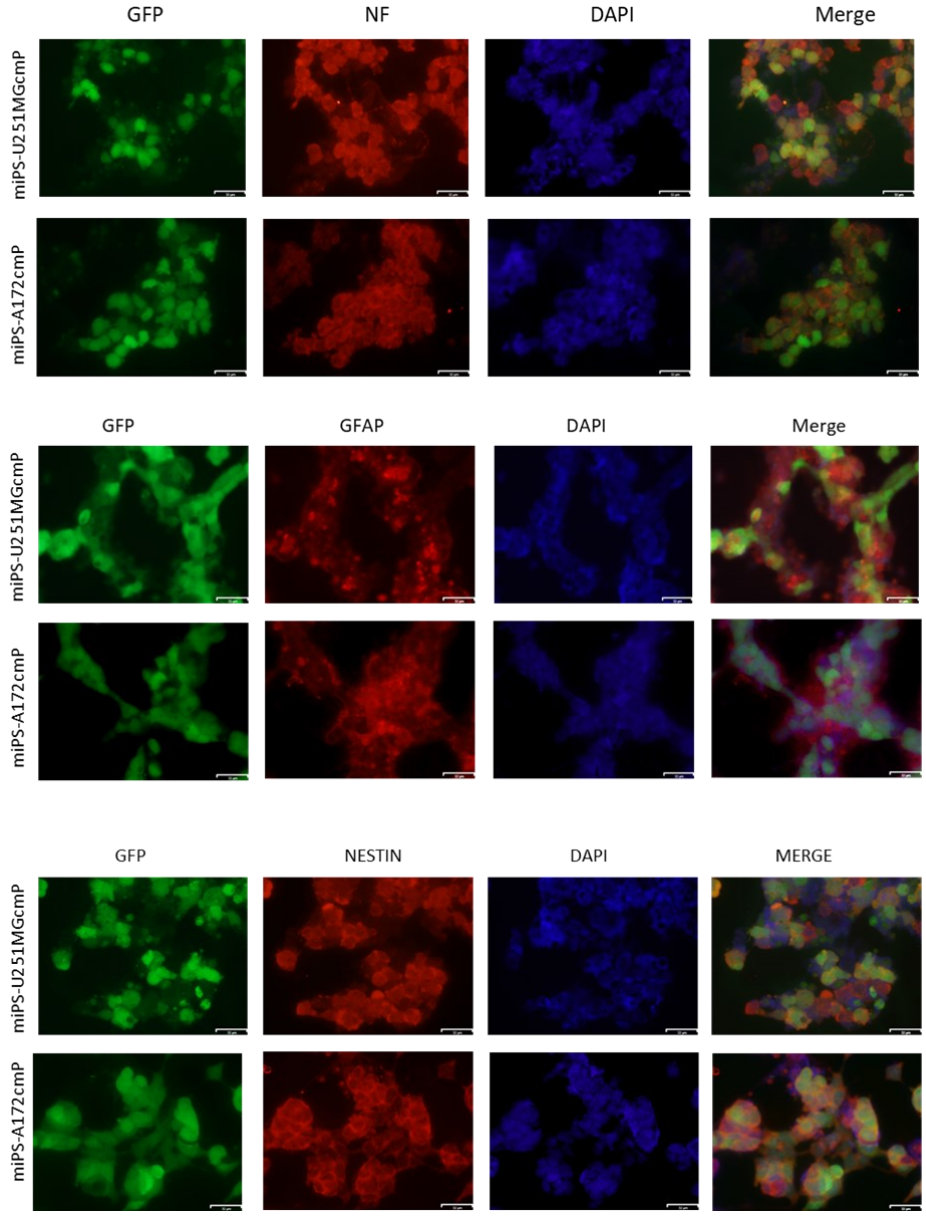

Figure 8: the Primary cells U251MGcmP and miPS-A172cmP also cells expressed GFAP and Neurofilament and NESTIN antibodies.

Discussion

We tried out two different condition media for treating the miPS cells obtained from GI1, U251MG and A172cell lines. After 3 weeks 50% condition media the cells shared features of Neuronal and glial cells with prominent structures of Axons, dendrites, and dendrites. The cells miPS-A172CM and miPS-U251MGcm cells were positive for GFAP, NESTIN and Neurofilament-2. Next, we tried to assess tumorigenicity of the cells in vivo in subcutaneous. CD44 is an adhesion molecule that binds to extracellular matrix, from these tumors, expression of several genes was evaluated in the sections. The expression of SOX2 was simultaneously found in the section of tumor (Figure 4). These results are consistent with the results of gene expression in vitro (Figure 1-3). The tumor sections are positive for NESTIN, GFP, SOX2 and Nueurofilament-2. Upon H and E staining the tumor sections showed mitotic bodies, narcosis and These results indicate the tumor composed of undifferentiated cells may exhibit rapid growth and big size in a short period. Under 2D culture conditions the miPS-U251MGcmP cells and the miPS-A172cmP cells showed features like Primary cells miPS-U251MGcmP cells showed positive marker for CD44 and CD133. CD44 has been suggested as a cancer stem cells (CSCs) marker. However, several clinical studies have indicated that CD44 low glioma cell exhibit CSCs traits. Immunofluorescence seems to be very low in the cells. Both cells miPS-U251MGcmP and miPS-A172cmP cells are positive for CD133. CD133 is a glycoprotein antigen found in normal and malignant tissues (Figure 5). CD133 is not only a biomarker for segregation and characterization of stem cells but may also have a role in cell growth, proliferation, and pathophysiology of the growing

tumors. Previous studies have shown that CD133-positive cells showed evidence of hypermutated and highly malignant sub-types of GBM. The cells form spheroids in vitro which confirm that the cells are maintaining stemness. At the same time the cells were positive for SOX2 immuno-staining (Figure 6). This confirms that the cells are expressing Stem cell like characteristics. We further tried to see if the cells were positive for the Neurofillament-2, GFAP and NESTIN. Gliomas are brain tumors that develop from glial cells found in the brain and spinal cord. GFAP is one of intermediate filament proteins and is specifically expressed in cells of the astroglial (astrocytic) lineage. Therefore, GFAP is widely used as an astrocyte marker in the brain, and glioma shows positive GFAP immunostaining. We confirmed the expression of GFAP by immunofluorescence in both primary cells A172cmP and miPS-U251MGcmP cells. At the same time when the cells were cultured in Matrigel the cells formed tube.

Conclusion

The GSCs converted from miPSCs suffice the definitions of CSCs as neuronal cells. since the cells can. This process of establishing CSC model will be useful for understanding the induction process of different CSCs in the future.

Future plan

Check for markers for GSC with qPCR. Perform Limited dilution assay to assess *in vito* selfrenewal potential. Employ DPI to on the primary cells to check if it is effective afainst GSCs.

Acknowledgement

A dissertation is a long journey. It's a long individual journey but unrealizable in solitude. For the past three years, since I started Ph.D. program in the faculty of Interdisciplinary Science and Engineering in Health systems, Okayama University 22nd April 2019. So many people have provided me with their essential support. Being here in Japan and especially getting used to the working environment was challenging. Family, friends, and colleagues have sustained me during this time. My family had been the piller of my strength and flaming source of inspiration during this whole journey. I want to thank my supervisor Professor Masaharu Seno for his consistent support and guidance during the running of this project. It has been an absolute honor to have been mentored by him. I want to express my gratitude to Professor Ferens L. M. Szekeres for his constant support during the whole doctoral program. Furthermore, Assistant professor Maram Zaharah and Akimasa Seno had been incredibly supportive of gaining technical skills. Also, Gamkin, Hassan, Said Affify, Kazuki Kumon, Hager Ali, Hager Mansour, Mona Seta, Hend Nawara were very kind to me and supported me constantly during the ups and downs of this treacherous journey. I would like to express my sincere gratitude Otsuka Toshimi Foundation Scholarship for funding my studies in Japan.

Life is hard in Japan, especially as a foreigner. I would like to express my special regards to Kazumi Hatta, Ken Inoue, and Naomi Kobayashi had supported to me in getting used to life in Japan, helping me escape lab, and teaching me how to enjoy life here.

My friends from Bangladesh Chowdhury Arif Jahangir, Salek Ahmed Sajib, Mahdi Zulfikar and Emdadul Haque Topu for constantly lifting me up and motivating to move forward.